PLAQUE BEHAVIOR CHARACTERISTICS AND REGROWTH OF PLAQUE IN DISEASED ARTERIES TISSUE DURING POST-CRYOPLASTY PROCESSES

A Thesis by

Men-Chi Hsieh

B.S.M.E., Wichita State University, 2003

Submitted to the College of Engineering
and the faculty of the Graduate School of
Wichita State University
in partial fulfillment of
the requirements for the degree of
Master of Science

May 2006

PLAQUE BEHAVIOR CHARACTERISTICS AND REGROWTH OF PLAQUE IN DISEASED ARTERIES TISSUE DURING POST-CRYOPLASTY PROCESSES

I have examined the final copy of this Thesis for form and content and recommend that it be accepted in partial fulfillment of the requirement for the degree of Master of Science with a major in Mechanical Engineering

_____

T. S. Ravigururajan, Committee Chair

We have read this Thesis
and recommend its acceptance:

_____

Kurt Soschinske, Committee Member

_____

Janet Twomey, Committee Member

DEDICATION

To my parents

ABSTRACT

Atherosclerosis is a leading cause of heart diseases and mortality around the world. Recently cryoplasty has emerged as a potentially effective method to treat atherosclerosis. Finite element heat transfer and mass transfer models are developed in ANSYS in this study. The heat transfer model analyzes the heat transfer within the atherosclerotic plaque and arterial wall during the cryopalsty procedure. The model is useful in predicting the transient temperature through diseased wall tissues. The measurements can be used to decide the required treatment procedure effectively for freezing the plaque with minimal damage to the healthy arterial tissues. The model investigates the parameters that may effect temperature distribution within the tissue during the ablative procedure. A mass transfer model is developed using ANSYS to study the pressure effects on molecular diffusion across the arterial wall and the permeability effects of endothelial membrane during the molecular diffusion process.

ACKNOWLEDGEMENTS

First, I would like to thank my advisor, Dr. Ravi, for his patience to guide me through this research from the beginning. Without him, this thesis could not have been completed. I also would like to thank the committee members, Dr. Soschinske and Dr. Twomey for their helpful comments and suggestion in this research. I would like to thank to all my friends surrounding me for their friendship and encouragement that kept me motivated. I want to specially thank to my friend, Anil, my best friend in graduated school. He always showed concern for my project and gave helpful suggestion. Finally, I would like to thank my parents and my dear sister back home for their understanding and support.

TABLE OF CONTENTS

Chapter Page

1. INTROUDUCTION…….....1

1.1 Structure of A Blood Vessel…….……2
1.2 Atherosclerosis…….…….4
1.3 Respond to Injury - A Hypothesis…...……..4
1.4 Restenosis……7
1.5 Introduction to Cryoplasty……7
1.6 Cryoinjury in Blood Vessel…….....8

2. REVIEW OF BIOHEAT MODELS…….….13

2.1 Pennes Bio-Heat Transfer Model……13
2.2 Chen-Holmes Model…….....14
2.3 Weinbaum-Jiji-Lemons Model……15
2.4 Small Artery Model…….…16
2.5 Applicability of Models……..17
2.6 Choice of Models for Cyoplasty Ablation…….....18

3. CRYOPLASTY SIMULATION…….…….. 19

3.1 Mathematical Model……...19
3.2 Thermal Properties of Blood and Arterial Tissue…….……..21
3.3 Geometry of Atherosclerotic Plaque…...……23
3.4 ANSYS Application.……....23
3.5 Numerical Experimentation……27
3.6 Optimize of Balloon Temperature and Treatment Time…….31
3.7 Types of Atherosclerotic Plaque and Its Thermal Characteristics……..34
3.8 Sensitivity Test……39
3.8.1 Effect of Metabolism Heat Generation……..40
3.8.2 Effect of Blood Perfusion Rate……..42
3.9 Convergence Test……47

4. MASS TRANSFER IN THE ARTERIAL WALL……..52

4.1 Role of Low Density Lipoprotein in Atherogenesis……..……..52
4.2 Effects of Pressure on Particle Deposition in Artery……..….54
4.3 Modeling Mass Transfer using ANSYS……..55
4.3.1 Theory……...…….. ……. 55
4.3.2 ANSYS Solution Methodology……..…59
4.3.3 Geometrical Model……60
4.3.4 Material Properties and Other Model Parameters……60
4.3.5 Boundary Conditions……61
4.3.6 Result……63
4.4 Effect of Transmural Pressure…….……...67
4.5 Effect of Permeability in Molecules Transport …….……72

5 REGROWTH OF PLAQUE DURING THE POST-CRYOPLASTY PERIOD……..74

5.1 A Comparison between Cryoplasty and Angioplasty…….....…74
5.2 Influence of Low Temperature on Biological Tissues……75
5.3 Modeling Plaque Regrowth Based on Biofilm Model…….....…76
5.3.1 Biofilm Model and Capability….……77
5.3.2 Plaque Growth Model……..80
5.3.3 Numerical Results……..82

6. CONCLUSION……...86

LIST OF REFERENCES…….……89

APPENDICES…….……96

A. ANSYS DESCRIPTION AND THEORY…...…….97
B. FINITE ELEMENT FORMULATION OF PENNES BIO-HEAT EQUATION…..99

LIST OF FIGURES

Figure Page

1.1 Structure of a medium size muscular artery……3

1.2 Response to an injury hypothesis……..6

3.1 Meshed model of arterial wall and plaque used in the ANSYS analysis…….…...26

3.2 Temperature contour plot of plaque and arterial wall at -10°C (>60 secs)…….29

3.3 Temperature distribution plot of selected nodes located at plaque and arterial wall at -10°C (>60 secs)…….30

3.4 Thickness variation of plaque with freezing temperature and time……..…….33

3.5 Temperature history plots of plaque-artery interface for different plaque models……37

3.6 Temperature distribution plot for different plaque types during the cryoplasty ablation…….…..38

3.7 Arterial wall temperature profile at temperature of -120°C for different metabolic rates (Q_m: 0, 140, 5540 w/m^{-3})……..41

3.8 Arterial wall temperature profile at temperature of -120°C for different blood perfusion rates (ω_b: 0, 0.0014, 0.0028, 0.0056 $m_b^3 m_t^{-3} s^{-1}$)……..……44

3.9 Plaque and arterial wall temperature profile at a balloon temperature of -120°C with no blood perfusion effect.……...45

3.10 Plaque and arterial wall temperature profile at a balloon temperature of -120°C with blood perfusion rate of 0.0056 $m_b^3 m_t^{-3} s^{-1}$ ……..…….46

3.11 Temperatures at select nodes for element size length equal to 0.5 in convergence

test…….49

3.12 Temperatures at select nodes for element size length equal 0.25 in convergence test…….50

3.13 Temperatures at select nodes for element size length equal 0.01 in convergence test…….51

4.1 Geometrical model of arterial wall in fully meshed used in the mass transfer analysis……...62

4.2 LDL concentration distribution within the arterial wall (one month status post-cryoplasty diffusion)…….64

4.3 LDL contour plot of concentration distribution within the arterial wall (one month status post-cryoplasty diffusion)…….65

4.4 LDL contour plot of concentration distribution within the arterial wall (six months status post-cryoplasty diffusion……..66

4.5 Effect of transmural pressure for LDL diffusion in the arterial wall after one month…….69

4.6 Flux through the arterial wall after one month diffusion……..70

4.7 Effects of pressure on inlet flux per unit area through arterial wall……...……71

4.8 LDL Diffusion rate into arterial wall assume different permeability of arterial wall……..73

5.1 Schematic of the steps in plaque formation…..…….79

5.2 Thickness of plaque growth as a function of time.……85

LIST OF TABLES

Table Page

3.1 Thermophysical Properties Used in ANSYS Modeling…….……..……22

4.1 Thermal Analog Conversion for Mass Transfer Modeling in ANSYS…..……...58

5.1 Parameters Used For Plaque Growth Model……..…….…….84

LIST OF NOMENCLATURE

a radius, m
c specific heat, J/kgK
C concentration, mol/L
D diffusivity, m^2/s
h convective heat coefficient, W/m^2-k
L element length, m
L_e equilibration length for countercurrent vessel, m
k thermal conductivity, W/mk
n number of vessels, cm^{-2}
Δp transmural pressure, mmHg
Pe Peclet number
q_m metabolism heat generation, W/m^3
Q heat generation per unit volume, W/m^3
r radial distance, m
t time, s
T temperature, °C
V convection velocity m/s
x distance, m
ρ density, (kg/m^3)
σ_Δ shape factor for the heat transfer between the countercurrent vessels
ω blood perfusion (kg of blood/m^3 of tissue-s)

SUBSCRIPTS

a artery
b blood
eff effective
l liquid phase
m metabolism
s solid phase
t tissue
ε ratio of the equilibration length to the actual length of the vessel

CHAPTER 1

INTRODUCTION

Balloon angioplasty and stents implantation are techniques widely used to open the blockage in artery caused by atherosclerotic disease. Atherosclerosis is known as artery disease where the plaque buildups on the arterial wall to narrow the lumen and block the blood flow. With continuously narrowing of the artery lumen, it may further increase in the risk factor which leads to cause heart attack or stroke followed by rupture of plaque [1]. Balloon angioplasty and stenting show some advantages over bypass surgery, however long term results showed that angioplasty has limitation to prevent restenosis. Restenosis occurs in 20-50% of patients after balloon angioplasty and in 10-30% of patients receiving a stent [2].

A new form of angioplasty called cryoplasty has been introduced to reduce the chance of occurrence of restenosis. Cryoplasty is a technique which combines the dilation force of balloon angioplasty with delivery of cold thermal energy to vessel wall. Initial clinical results revealed that the cryoplasty is essentially reducing the restenosis rate and cause less invasive to arterial wall injury responded to angioplasty [3].

Currently, the cryoplasty is designed as a treatment for femoro-popliteal arterial disease, type of peripheral arterial disease. Patients with femoro-popliteal arterial disease below knee may cause serious leg pain, loose ability to walk, in advanced stage, can lead to ulcers, gangrene, and amputation of legs [4].

Cryoplasty has shown a high potential to prevent restenosis, however the influence of temperature induced by cryoplasty to the arterial wall still remain unclear. Also, the possible factors which may affect temperature distribution on the plaque and arterial wall during

cryoplasty procedure need to be identified in assisting the cyoplasty technique to be performed in carotid or coronary artery in the future.

1.1 Structure of A Blood Vessel

The structure of artery is well known and has been described in many literatures [5-6]. Primary, arterial wall consists of three layers: the intima, media, and adventia. The intima consists of an endothelial cell monolayer that prevents blood, including platelets, leukocytes, and other element from adhering to the luminal surface [6]. The intima and media are separated by the internal elastic lamina (IEL), although this border is not clearly defined in some areas such as bifurcations, branch vessels, and curvatures. The media is comprised of smooth muscle cells, elastin, collagen, and proteoglycans. The media makes up the greatest volume of the artery and is responsible for most of its mechanical properties. The external elastic lamina separates the media from the adventitia, which is rich in loose connective tissue and contains fibroblasts, vasa vasorum and nerves. The adventitia, the outer layer of artery, is made up of collagen, nerves, fibroblasts, and some elastin fiber. The adventitia contributes to the mechanical properties primary by facilitating tethering to the surrounding tissue.

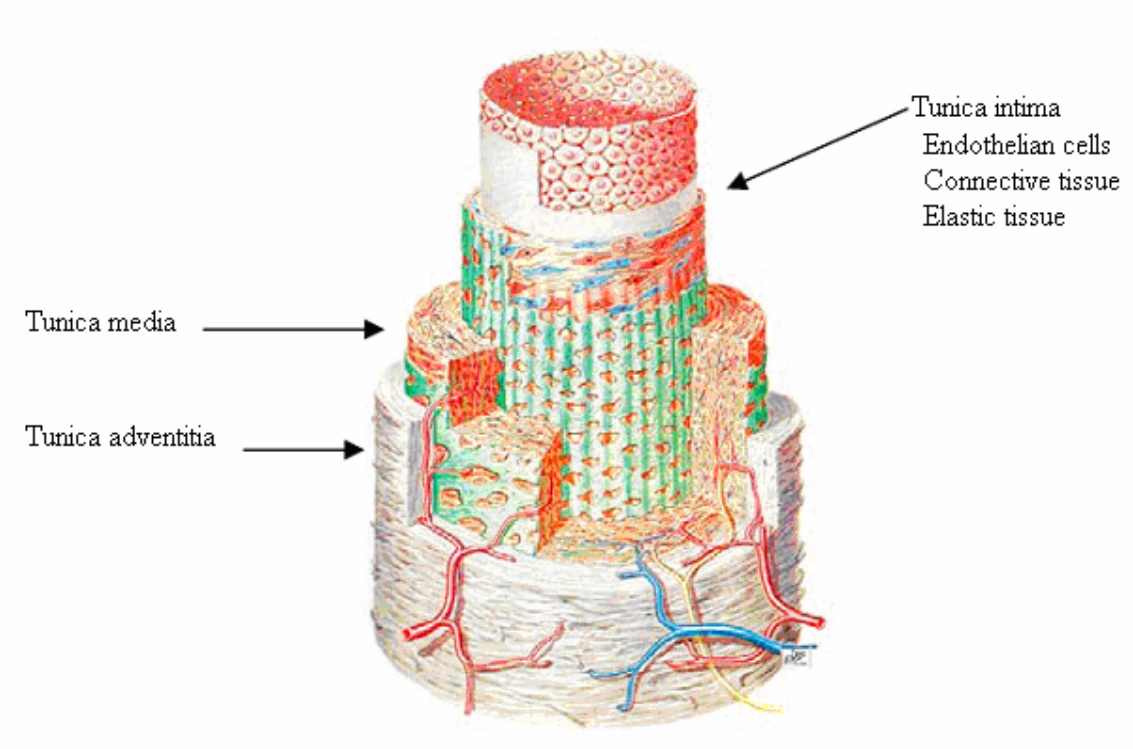

Figure 1.1 Structure of a medium size muscular artery [5]

1.2 Atherosclerosis

Atherosclerosis is a serious disease affecting arterial blood vessels. It is generally referred to as hardening or thickening the arteries. Atherosclerosis involves the slow buildup of deposits of fatty substances, cholesterol, and other materials in the lining side of an artery. The buildup deposit normally referred to as plaque, which can partially or totally block the blood flow in the lumen, leading to damage of the tissue downstream which has lost needed blood flow.

The most dangerous result from atherosclerosis is rupture of the plaque. When plaque ruptures, fatty contents of plaque are released into the blood stream. This fatty mass may travel through the bloodstream and block somewhere in the downstream of the blood vessel. Most often, the rupture of plaque triggers the formation of a blood clot thrombus, which can further narrow the lumen or even block the artery [1]. When the artery is blocked in sudden, it may cause a heart attack or stroke.

1.3 Response to Injury - A Hypothesis

Factor which triggers the atherosclerosis in the first place is not completely understood yet. However, during the past decades increasing the knowledge of this complex process, researchers have come up several hypotheses. These include the response to the injury hypothesis [7], the lipid infiltration hypothesis [8], the oxidation hypothesis [9], and the inflammation hypothesis [10]. Among these, response to injury hypothesis is the most accepted concept.

According to response to injury hypothesis atherosclerosis is considered as a chronic

inflammatory response of arterial wall, initiated by some form of injury to the endothelium. Sequence of the events in development of atherosclerosis lesion is shown in Figure 1.2. The tasks are summarized below:

(1) Development of focal regions of chronic endothelial injury. The main factors that could induce this injury include: hyperlipidemia, hypertension, smoking, homocystein, homodynamic factors, toxins, viruses, immune reactions.

(2) Chronic endothelial injury results in endothelial dysfunction, which includes increase membrane permeability, increase leukocyte adhesion and emigration. Lipoprotein stick to endothelial surface, get oxidized and insudate into the vessel wall.

(3) Smooth muscle cells migrate from media to intima. Monocytes differeinciate to momacrophages and get activated. Insudation of lipids continues

(4) Macrophages and smooth muscle cells engulf oxidized lipids and become foam cells

(5) Smooth muscle cells proliferate and actively synthesize collagen and proteoglycan. Increase in both extracellular and intacellular lipid deposition.

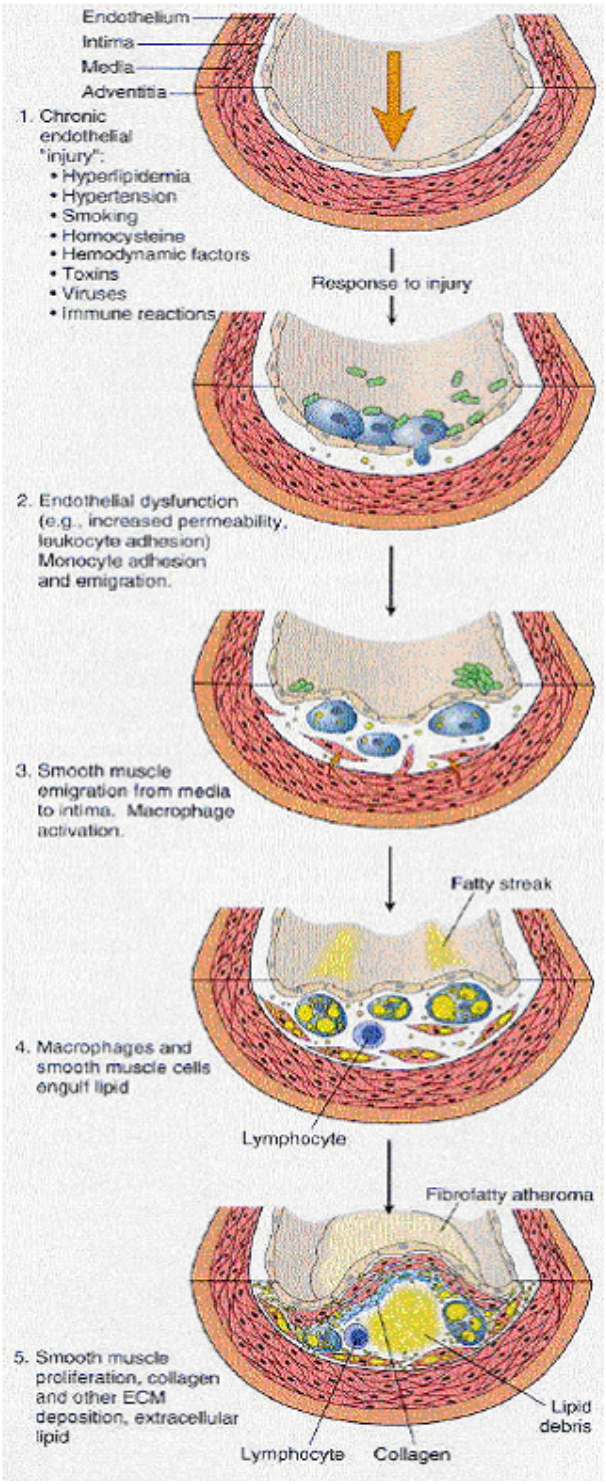

Figure 1.2 Response to the injury hypothesis [7]

1.4 Restenosis

Restenosis is the major problem limits the balloon angioplasty. Each year, more than 800000 angioplasty procedures are performed in United States, however, with 30%-50% of these resulting in restenosis [2]. Restenosis occurs when the lumen renarrow again at the treated vessel in the following months of patients who received angioplasty. Restenosis is a complex process which involves several mechanisms [11].

The first mechanism of restenosis is “elastic recoil”, elastic fibres of vascular wall to overstretching by balloon catheter, tend to spring back immediately after the procedure. The second mechanism is chronic remodeling, in which the vessel wall slowly contracts as it heals, thus producing a smaller lumen. The third mechanism of restenosis is neointimal hyperplasia, which involves proliferation of smooth muscle cells inside the internal elastic lamina and migration of smooth muscle cells into the intima.

1.5 Introduction to Cryoplasty

Angioplasty has been used as an effective procedure to open the clogged artery and restore blood flow. However, restenosis occurs in 30%-50% of the patients after balloon angioplasty in 3 to 6 months period [2]. To prevent retenosis, normally a wire mesh stent is implanted at the disease siege after angioplasty. Implantation of stents improves reduction in the patency rate of restenosis. However, scar tissue form and buildup inside the stent due to aggressive neointimal response that stents generated, will finally grow through the wire of stent and narrow the lumen of artery again [12].

A new form of angioplasty, called cryoplasty has been introduced to improve the results

typically associated with angioplasty. Cryoplasty is known as a technique which combines dilation force of balloon angioplasty with delivery of cold thermal energy to the vessel wall.

Cryoplasty procedure is very similar to balloon angioplasty. A catheter is threaded into the area of the artery that is clogged. However, nitrous oxide is used instead of saline solution to inflate the balloon. This process proposed is gentler on the artery wall than angioplasty; preventing much of the inflammation and scarring that contribute to restenosis to renarrowing of the vessel [13].

Cryoplasty is performed by using a PolarCath device designed by CryoVascular Systems, Inc. Patient is awake during the therapy. The physician makes an opening in a patient's groin, and a catheter is threaded into the blocked artery. Once the catheter reaches the blockage area, the highly compressed liquid nitrous oxide flows through the lumen of the catheter to the balloon. Due to the pressure difference, the nitrous oxide changes its liquid state to gas state instantaneously. Temperature inside balloon rapidly decreases and cools the plaque to the desired temperature while the balloon expands and opens up the blockage.

After the procedure, the nitrous gas is exhausted back to the cryoinflation unit and the balloon deflated. The whole process is complete within 60 seconds. Angiogram is performed to examine the blood flow after therapy.

1.6 Cryoinjury in Blood Vessel

Cryosurgery has been used extensively to treat the tumors and diseased tissue of the body. In vivo and in vitro assessment has a long history in tumor tissue, but there is limited knowledge about the cryotherapy on vascular tissues. When cryotherapy is performed in

human blood vessel, the safety of cryotherapy and cryoinjury responded by the blood vessel are concerned.

In Gage et al [14] study, they froze dogs' arteries, veins, and biliary structures by wrapping a surgical tube around each conduit and circulating extremely cold liquid nitrogen about -140°C through the tube for ten minutes. This procedure resulted in full thickness freezing. The treated arteries regained normal conduit function immediately after the circulating blood thawed the vessel. Thus, demonstrated that arterial structure have a benign histological response to cold thermal energy with no interruption in conduit function.

While healing process occurs in blood vessel after freezing and thawing. Smooth muscle cells regenerate rapidly, and intimal hyperplasia results in some narrowing of the lumen. The remodeling is facilitated by pressure within the vessel, and intima hyperplasia tends to regress over the following months [14].

Hollister et al. [15] examined the response of monolayers of human smooth muscle cells and endothelial cells to freezing. The results of their work showed that smooth muscle cells were more sensitive to cold injury than endothelial cells, with different evident in the temperature range of 0 to -15° C.

An in vivo study by Cheema et al. [16], working on rabbits, comparing effect of cryotherapy on vessel after iliac arterial balloon angioplasty with balloon angioplasty alone, showed no late beneficial effects from freezing on the diameter of the lumen. In this study, intimal hyperplasia and collagen formation were increased by the cryotherapy. The average vessel wall temperature was cited as -26° C. Gage [14] gave comment on this study, he addressed that -26° C was probably too cold to permit any benefit in term of a selective

cellular response. However, he also pointed out that the main problem is that the temperature that might produce a modified response in the muscle cells and elastic and collagen fibers *in vivo* is still not known. He further suggested that if benefit is to be achieved by cryotherapy, the tissue temperature should be in the range -10 to -15° C.

James et al. [17] clearly defined the cryoplasty goal. Freezing technique is used to control the smooth muscle response to injury by the balloon angioplasty. The goal of cryopalsty is to induce apotosis in the vessel wall, which is thought to inhibit smooth muscle proliferation, rather than destroy the muscle tissue. Apotosis is known as a natural biological mechanism that results in removal of unwanted tissue via programmed cell death [3]. Experimental tests on human artery smooth muscle cells was found that the peak of apotosis occured at -10°C and no apotosis was observed above -5°C [17].

Safety of cryoplasty system has been evaluated by Terashima et al [18] on animal models *in vivo*. 19 porcine coronary arteries were subjected to freezing in a temperature range of -5°C to -10°C for 25 seconds using a cryoplasty device. Their results showed that the health of animals were not impacted by the cryotherapy treatment as indicated by clinical and physiological evaluations. The results were also compared with animals subjected to traditional balloon angioplasty, and found that the percent diameter of stenosis in the cryoplasty group was less than that of the angioplasty group up to a 183 day investigation.

In vivo studies have demonstrated the potential of cryotherapy to prohibit restenosis processes. However, the mechanisms of injury during cryoplasty and appropriate treatment thresholds are not well known. In this case, the animal in vitro models may provide important information on thermal parameters and mechanisms of injury. Animal in vitro models are

widely used in experiments, because it is easy to obtain and is cost effective. Moreover, it is important to carefully choose the model system for in vitro work on cryoinjury characterization to adequately match the clinical situation. Bischof et al [44] have looked at the in vitro models with smooth muscle cells to determine the appropriate system for examining the cryoplasty mechanisms. Rat and pig smooth muscles were compared to human smooth muscle cells to determine whether either species exhibited the similar responses to human. In addition, they further compared the response of the smooth muscle cells embedded in suspension, in collagen and fibrin to determine the effect of the cellular environment. The freezing temperature cited in this study was -80°C and the duration of the freeze was 10 minutes. The test samples were then thawed at a room temperature of 37°C for 0 to 3 days for observation. Under all cellular environments, their test results showed that the pig smooth muscle cells behave similarly to the human smooth muscle cells, whereas rat smooth muscle cells appeared less sensitive with a higher rate of survival to cooling at a fast rate in suspension. Another important result in this study was that human smooth muscle cells were found to be less sensitive to temperatures at -11°C when embedded in collagen, only 30% of the cells survived compared to a 70% survival rate in suspension. Their results suggested that the model including the fibrin may be a more appropriate model for testing treatment for restenosis than the collagen model; this is because cell proliferation is an important part of restenosis. When collagen is known to inhibit smooth muscle proliferation, it may not be appropriate for testing treatment for restenosis in the collagen model [44, 45].

Researchers have investigated the arterial wall characteristics to explore the possible pathologies of atherosclerosis to explain how plaque buildup blocks the lumen of human

blood vessel. The mechanisms of restenosis resulted from the pressure induced by the balloon angioplasty technique. More researches were performed to seek the mechanisms of injury response of arterial wall tissues on both smooth muscle cells and enthodial cells by freezing, when cryoplasty shows potential to combat restenosis process. However, the characteristics of plaque are different from the arterial tissue. A more appropriate model system for testing the treatment for restenosis should combine both arterial tissue and plaque together rather than test on each alone. However, attempts to perform measurements of in vivo in the human body is not easy, especially since most of them are not invasive. In this case, finite element method may appear as a useful tool to provide some important information based on physiological conditions when the parameters of arterial, plaque and blood flow are known.

The main objectives of this thesis are:

1. Establish transient temperature distribution in the arterial wall and plaque as a function of cryogenic fluid temperature.
2. Analyze the influence of blood perfusion and tissue metabolism on the arterial wall and plaque temperature distribution.
3. Study the re-growth of plaque during the post-cryoplasty period based on biofilm growth model.

CHAPTER 2

REVIEW OF BIOHEAT MODELS

2.1 Pennes Bio-Heat Transfer Model

Heat transfer in living tissues is often influenced by the blood flow through the vascular system. When there is a significant difference between the temperature of blood and the tissue in which blood flows through, convection heat transfer dominates. Researchers have proposed many different models to dates for different applications [19- 22], due to different effects of the blood.

The first comprehensive heat transfer model for blood perfusion was developed by Pennes in 1948 [19]. His simple model considered the effects of perfusion using a source-sink relationship between the vessels and the tissue. The model was characterized by the following equation often referred as ”the bio-heat transfer equation”.

$$\rho c \frac{\partial T}{\partial t} = \nabla(k \nabla T) + \omega \rho_b c_b (T_a - T) + q_m \tag{2.1}$$

It is not difficult to see that Pennes’s bio-heat equation is simply Fourier’s law with two additional terms. The second term on the right hand side of equation describes the heat transfer between the blood and tissue and the last term is the rate of heat generated by tissue due to metabolism. The main assumption behind this model was that the vessel temperature was constant and the heat transfer took place predominantly in the capillaries. No importance was given the vascular structure of tissue and blood flow direction. The model assumes that the arterial blood enters the capillary bed at certain temperature (T_a) and instantaneously equilibrates with tissue temperature, and leaves tissue at temperature, T.

Over the years, Pennes bio-heat equation has been investigated widely under criticisms. However, it was also shown that much of the discrimination that has been directed toward Pennes model is not justifiable [23].

2.2 Chen-Holmes Model

In 1980, Chen and Holmes [20] presented a more detail equation with the effect of the blood vessel dimensions taken into account. Basically, their model questioned the perfusion term in Pennes equation. They defined a" thermal equilibrium length" (L_e), which is the length at which the difference between the blood and tissue temperature decreases to 1/e of the initial value. Their analysis of blood vessel and their equilibration showed that Pennes' model is conceptually incorrect from the point of view of complete equilibration at the capillary level. Their analysis indicates that the heat exchange between the tissue and the vessels occurs also before the capillary level. In their model, they proposed that larger vessels be modeled separately from small vessels and tissue. They developed three terms to replace perfusion term in Pennes model for heat transfer based on their analysis. Each term modeled a different region of tissue. The bio-heat equation was modified as:

$$\rho c \frac{\partial T}{\partial t} = \nabla \cdot k \nabla T + (\rho c)_b \omega^* (T_a^* - T) - (\rho c)_b \bar{u} \cdot \nabla T + \nabla \cdot k_p \nabla T + q_m \qquad (2.2)$$

The second term on the right hand side $(\rho c)_b \omega^* (T_a^* - T)$ is the same as Pennes' equation except the perfusion ω^* and arterial temperature T_a^* is specific to the volume being considered. The third term is the heat transfer contribution of blood, which is equilibrium with tissue. $\bar{u}$ is the blood velocity vector as it diffuses through a porous tissue. Finally, the fourth term is to account for contribution of the nearly equilibrated blood in a tissue

temperature gradient. The nearly equilibrated blood contributes to small temperature fluctuations within the tissue and the effect is modeled as the tensor "perfusion conductivity":

$$k_p = n(\rho c)_b \pi r_b^2 \overline{V} \cos^2 \gamma \sum_{i=1}^{\infty} \frac{L_e}{L_e^2 \beta_i^2 + 1} \tag{2.3}$$

k_p is a function of local averaged blood velocity vector ($\overline{V}$), relative angle (γ) between blood vessel direction and the tissue temperature gradient, the number of vessels (n), and the vessel radius (r_b). The Fourier integral spectral wave number (β) can be approximated as the inverse of vessel length.

The assumptions in this model include: (1) neglecting the mass transfer between vessel and tissue space, and (2) treating the thermal conductivity and temperature within the tissue-vessel continuum as that of solid tissue since the vascular volume is much smaller than that of the solid tissue.

The limitation of this model is not difficult to be observed. The given details required make this model not easy to implement. Especially, the "perfusion conductivity" term is difficult to evaluate.

2.3 Weinbaum-Jiji-Lemons Model

In 1984, Weinbaum, Jiji and Lemons came up with a model that took into account the vasculature. The model developed by Weinbaum et al. [21] was different from the earlier models by Pennes and Chen-Holmes from the aspect from addressing the issue of countercurrent nature of arteries and veins. From their observations of the vasculature of the rabbit thigh peripheral tissue, they concluded that the local blood contribution to heat transfer is mainly associated with an incomplete countercurrent heat exchange mechanisms between

paired arteries and veins rather than the capillary perfusion.

The main assumptions of their model were (1) the tissue temperature was the mean of the arterial and venous blood temperatures and (2) heat from the artery of a vessel pair is almost completely conducted to the vein. The model based on an effective conductivity which can have a tensor representation and which incorporates the effect of blood flow based on vascular data and counter flow heat transfer analysis has the form:

$$\rho c \frac{\partial T}{\partial t} = \frac{\partial}{\partial x}\left(k_{eff} \frac{\partial T}{\partial x} \right) + q_m \tag{2.4}$$

where k_{eff} is the effective conductivity. In the one dimensional case where the blood perfusion is in the direction of the temperature gradient, the effective conductivity is expressed as:

$$k_{eff} = k\left[1 + \frac{n\left\{ \pi r_a^2 (\rho c)_b \overline{V} \cos\gamma \right\}^2}{\sigma_\Delta k^2} \right] \tag{2.5}$$

where n is number of vessel, $\overline{V}$ is blood velocity vector, γ is relative angle between the blood vessel direction and the tissue temperature gradient, and σ_Δ is the geometric factor for the heat transfer from an artery-vein pair to the tissue.

The limitation of this model is that it is strongly dependent on the local blood vessel configuration and requires detailed physiological data for the appropriate analysis. However, the detailed information about vascular geometry is not always available. Another known limitation of this model is that it applicable in situation where equilibration constant ($\varepsilon = L_e/L$ ratio of the equilibration length to the actual length of the vessel) $\varepsilon << 1$.

2.4 Small Artery Model

The small artery model was developed by Anderson (1991) in studies of the kidney

cortex [22]. The finite difference small artery model considers the energy balance in a control volume (i, j, k) which contains either an artery or a vein. For an artery parallel to z-axis, the equation is

$$Q_a = N(VA)_a(\rho c)_b(1+\lambda-2\lambda\xi)\left(\frac{T_z - T_{z-\Delta z}}{\Delta z}\right) \tag{2.6}$$

and for a vein

$$Q_v = M(VA)_v(\rho c)_b(1+\lambda-2\lambda\xi)\left(\frac{T_{z+\Delta z} - T_z}{\Delta z}\right) \tag{2.7}$$

where N and M are the density of interlobular arteries and veins in the kidney cortex, respectively. V is the mean velocity and A is the cross section area of vessel. ξ is the fraction of the total interlobular artery flow within the control volume; in the kidney cortex, ξ =1 at the cortico-medullary junction and decrease to ξ =0 at the outer capsule. The bleed-off is presented by the λ term, where λ =1 presents complete bleed-off. Numerical implementation of this model is straightforward and simple when the vessel density within the tissue region of interest is known.

The main assumptions of this model include: 1) thermal equilibration length within the volume is much less than the actual vessel length, 2) bleed-off is uniform along the length of vessel, 3) bleed-off is modeled as a varying flow along the vessel, 4) bleed-off heat transfer is negligible, 5) there are no major thermally significant vessels in the region. The model has been shown to be valid in the canine kidney cortex where there is uniformly oriented counter-current artery vein architecture of 70 μm diameters.

2.5 Applicability of Models

There have been studies comparing the applicability of different models in different regions. Hybrid models using a different model for different regions have come up because of the failure of a single model to account for heat transfer in all regions. A comparison of different models has been done by Arkin et al. in 1994 [24]. They suggested that no single equation being able to provide a complete description of heat transfer process in tissue in different regions, and thus suggested the use of a combination of equations.

2.6 Choice of Models for Cyoplasty Ablation

In this research, Pennes model have chosen to study cryoplaty ablation. Pennes' model was chosen because of its simplicity and it is the most widely used model for living tissue heat transfer analysis. During the cryopalsty ablation, the blood flow in the main artery is essentially blocked by the inflated balloon. However, the blood in the small arteries surrounding the arterial wall still allowed to flow through the arterial tissue within the control volume interested. The diameter of small artery is about 175 μm and the equilibration length ratio measured by Chen and Holmes is around 1 [46]. This means that the blood in small artery will fairly equilibrate with the tissue temperature within the control volume. Along with Xu's observations in porcine kidney [47], Pennes' model appears to be applicable to regions where the vasculature comprised of numerous small thermally significant vessels where $\varepsilon \approx 1$. This provides us some confidence to make Pennes model as appropriate model in this study. Most important is that numerical solution of Pennes's bio-heat equation can be solved easily either by finite difference or finite element method.

CHAPTER 3

CRYOPLASTY SIMULATION

3.1 Mathematical Model

Heat transfer in smooth muscle tissue within the artery wall is governed by the bioheat equation [19]:

$$\rho_t c_t \frac{\partial T}{\partial t} = \nabla(k_t \nabla T) + q_b + q_m \tag{3.1}$$

where T is the tissue temperature, t is the time, k is the thermal conductivity of tissue, ρ and c refer to the tissue's density and specific heat coefficient respectively. Also, q_m is the rate of metabolic heat generated by the tissue and q_b describes the energy transfer between blood and tissue suggested by Pennes that

$$q_b = \rho_b c_b \omega_b (T_b - T) \tag{3.2}$$

where ρ_b and c_b are blood density and specific heat coefficient respective, ω_b is the blood perfusion rate and T_b is the temperature of artery blood.

Therefore, the equation can be rewritten as:

$$\rho_t c_t \frac{\partial T}{\partial t} = \nabla(k_t \nabla T) + \rho_b c_b \omega_b (T_b - T) + q_m \tag{3.3}$$

Assume that the time-dependent temperature profile depends on radial position only, the equation (3.3) can be reduced to

$$\rho_t c_t \frac{\partial T}{\partial t} = k_t \frac{1}{r} \frac{\partial}{\partial r}\left(r \frac{\partial T}{\partial r} \right) + \rho_b c_b \omega_b (T_b - T) + q_m \tag{3.4}$$

the above equation must be solved with the following initial and boundary conditions:

$t = 0, \quad T = 37°C \quad$ for all r

$r = 0, \quad T = T_s \quad$ for all $t > 0$

$r = \infty, \quad T = 37°C \quad$ for all $t > 0$

where r is the radial distance through the arterial wall and T_s is the surface temperature of plaque once the cold from the balloon is applied. Initial model temperatures are uniform at 37°C. The outer layer tissue temperature is maintained at the human body temperature (37°C).

A 2-D finite element heat transfer model is developed in ANSYS to solve the bio-heat equation. Some appropriate boundary conditions and assumptions are made as follows:

(1) The atherosclerotic plaque is modeled as eccentric and circular, which is embedded in a circular artery. The heat conduction transfer through the arterial wall is assumed in radial direction only.

(2) The arterial wall and plaque tissues are assumed to be homogenous, the tissue thermal properties of artery and plaque are constant and independent of temperature.

(3) The initial temperatures of artery and plaque were uniform at 37°C.

(4) The temperature of outer arterial wall was maintained at 37°C at all times. (In short time freezing period, this assumption is reasonable)

(5) The temperature of blood perfuse the tissue was 37°C.

(6) The rate of blood perfusion is independent of temperature.

(7) The balloon was modeled with no thickness and no resistance of heat transfer, where the surface temperature of plaque in contact with balloon surface is same as the nitrous oxide temperature.

(8) The temperature and pressure of gas in the balloon remains constant.

(9) No phase change occurs within the tissues during the cooling process

Equation (3.4) was solved with the finite element method by available commercial finite

element package ANSYS in 2-D presentation, the details of model description and procedure will discuss later in this chapter.

3.2 Thermal Properties of Blood and Arterial Tissue

Thermal properties of blood are well known and have been widely used in skin burn models [25]. Thermal properties of human arterial tissue and plaque were measured by Valvano et al [26]. They measured tissue thermal properties as a function of temperature using a thermistor heating technique. The measurements were performed at 35, 55, 75, 90°C respectively. Thermal conductivity and diffusivity of tissues increases as temperature increases. These values used in current model analysis maybe somehow inappropriate. Tissue experience a phase change in low temperature environments, also the thermal properties of frozen tissue and tissue above sub-zero are largely different. However, thermal properties of arterial tissue below sub-zero were not cited in literature. To simplify the problem, parameters measured by Valvano [26] at 35°C were used in current modeling. The completed set of thermal properties of blood and tissue used in modeling are listed in Table 3.1.

TABLE 3.1

THERMOPHYSICAL PROPERTIES USED IN ANSYS MODELING

Tissue Type	Thermal Conductivity(W/m°C)	Specific heat coefficient(Jkg/°C)	Density (kg/m^3)
Average Plaque[26]	0.490	2984	1450
Fatty Plaque[26]	0.484	2849	1450
Fibrous Plaque[26]	0.485	3014	1450
Calcified Plaque[26]	0.502	3089	1450
Arterial Wall[27]	0.432	3340	1060
Blood[25]	0.5	3500	1080

3.3 Geometry of Atherosclerotic Plaque

It is difficult to determine the atherosclerotic plaque geometry commonly found in the artery, since any geometry of plaque configurations are possible. In a finite element analysis of balloon angioplasty, Kleinberger et al. [28], reviewed the histological record of patients who died of heart disease relating to atherosclerosis, and grouped the geometry of atherosclerotic plaques into three basic configurations; concentric and circular, eccentric and circular, eccentric and non-circular. The model for concentric and circular plaque embedded in the circular arterial wall was used in this study.

3.4 ANSYS Application

The heat transfer model based on Pennes's bioheat equation of arterial wall during the cryoplasty application is solved numerically in ANSYS. The commercial finite element package ANSYS is installed on a Pentium computer in the computer laboratory located at the Wichita State University engineering building.

In the first step in ANSYS, we generated the circular shape of the arterial wall with assume that the artery has an average thickness of 1mm and 4mm lumen in diameter. Then, we added the plaque layer with a thickness range from 1 mm to 3 mm. Though, our initial interest is modeling a layer-specific arterial wall, as we know the arterial wall is composed mainly of three layers: intimal, media and adventia. However, this idea had to be fold since no thermal properties of these three layers has been specifically reported yet. Furthermore, due to the thinness of the arterial wall, it is reasonable to assume the three layers have similar thermal properties.

Once the model is developed in ANSYS, the second task is assign proper material properties and finite element type into our model for simulation. The thermal properties in both artery and plaque are assumed to constant and independent of temperature. It is very important to notice that when assign thermal properties into model, all the data we enter should have the consistent units. For example, if we decide use meter as our model length scale, then all the parameters' dimension involves length should convert into meter scale. Since there is no default unit in ANSYS, any consistent system of units are accepted. Failed to maintain consistent units may result inaccuracy of solution.

ANSYS provides two finite elements for 2-D steady-sate or transient thermal analysis; they are 4-nodes PLANE 55 and 8-nodes PLANE 77. Both finite elements are well describe our model, but PLANE 55 showed lack of coverage of our model when mesh was performed, this may due to complex shape of model, so we picked PLANE 77 as our model simulation. The element descriptions of PLANE 55 and PLANE 77 are well documented in ANSYS element reference manual.

For mesh generation, ANSYS mesh tool was used and the smart size control was set for fine generation for both arterial wall and plaque regions. Apparently, smaller the size of element to generate the mesh, more computing time is required. A fully meshed of the model is shown in Fig 3.1. The model consists of 4182 nodes and 1314 8-nodes thermal elements. The outer annulus of model presents the arterial wall and the inner annulus referred as plaque tissue respectively. The hole in the center of the model was simulated as the cryoplasty balloon with nitrous oxide gas fulfilled in it.

An initial temperature condition of 37°C was applied uniformly in all nodes within the

arterial wall and plaque boundary. On the boundary of the outer arterial tissue, a constant temperature condition corresponding to the initial body temperature was maintained at 37°C all the time. Balloon fluid temperature was applied on the inner surface of the plaque boundary, as well as the convective boundary condition due to blood perfusion.

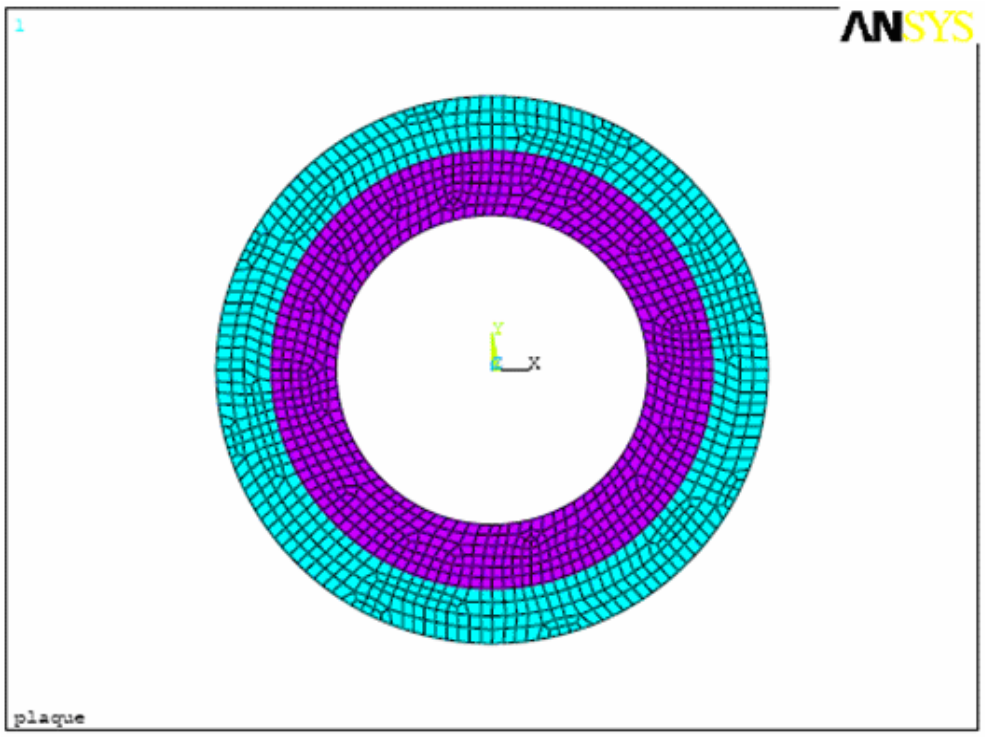

Figure 3.1 Meshed model of arterial wall and plaque used in the ANSYS analysis.

3.5 Numerical Experimentation:

The initial result was solved by applying -10°C, standard balloon temperature used in cryoplasty to freeze the plaque which has 1 mm thickness for 60 seconds. The temperature history plot of various nodes located along the radial direction is shown in Figure 3.2. Temperature rapidly decreased in the arterial wall and heat transfer balanced within a very short time of about 24 seconds. This is due largely to the affect of boundary condition constrained to 37° C. The lowest temperature achieved in the node located between plaque and normal tissue is 10°C, if the cryoplasty goal is to freeze plaque to a temperature range from -5°C to -15°C to turn liquid like plaque into solid state and induce apoptosis, the temperature result in this model maybe insufficient to kill the abnormal tissue. It was found that apoptosis will not occur in tissue for temperatures warmer than -5°C [17].

This result suggested that a single treatment temperature may be difficult to overcome different plaque thickness. The thicker plaque is expected to require lower treatment temperature for the ablation. This can be achieved by either increasing the balloon pressure to allow more nitrous oxide to flow into the balloon to compress the plaque and push it back against the arterial wall even further or apply cooler balloon temperature to freeze the plaque.

However, further increase balloon pressure is not a good option since it may cause possible overstretch to the arterial wall and trigger the smooth muscle cells proliferation, migration of those cells from media to intima, which was believed to be the main reason to cause restenosis response to injury by balloon angioplasty [29]. Control temperature maybe a good alternative, but it is not without any difficulty. Prediction of freezing propagate in arterial wall has to be known as well as the freezing time. This is to assure the plaque is

completely frozen to the desired ablation temperature while minimizing the damage to the surrounding healthy arterial tissue.

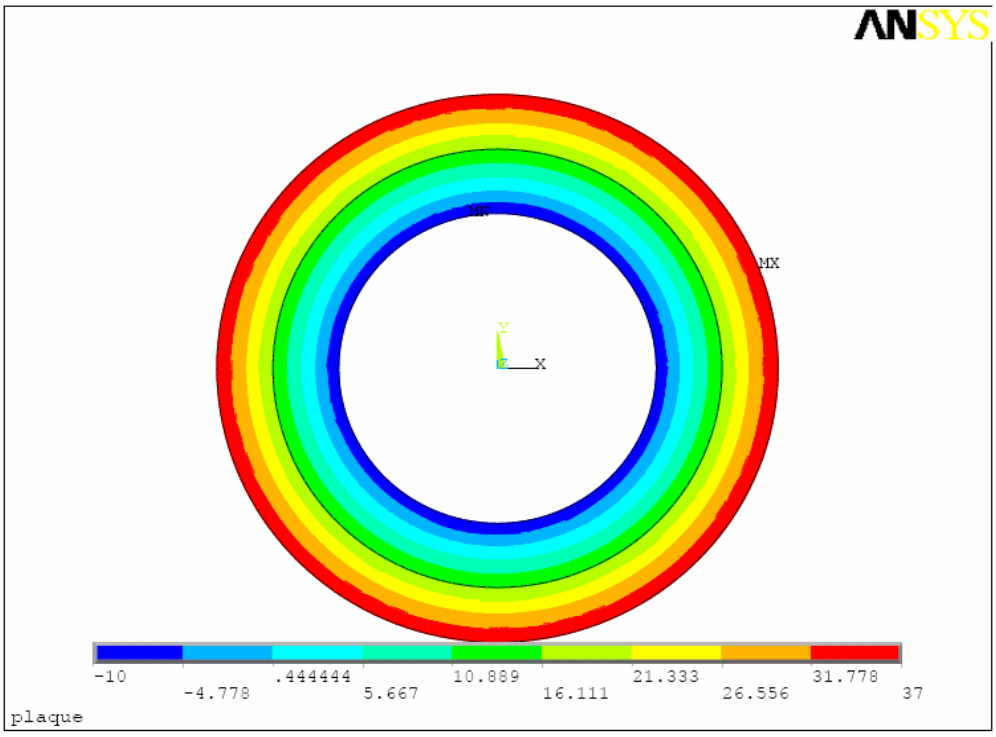

Figure 3.2 Temperature contour plot of plaque and arterial wall at -10°C (>60 secs).

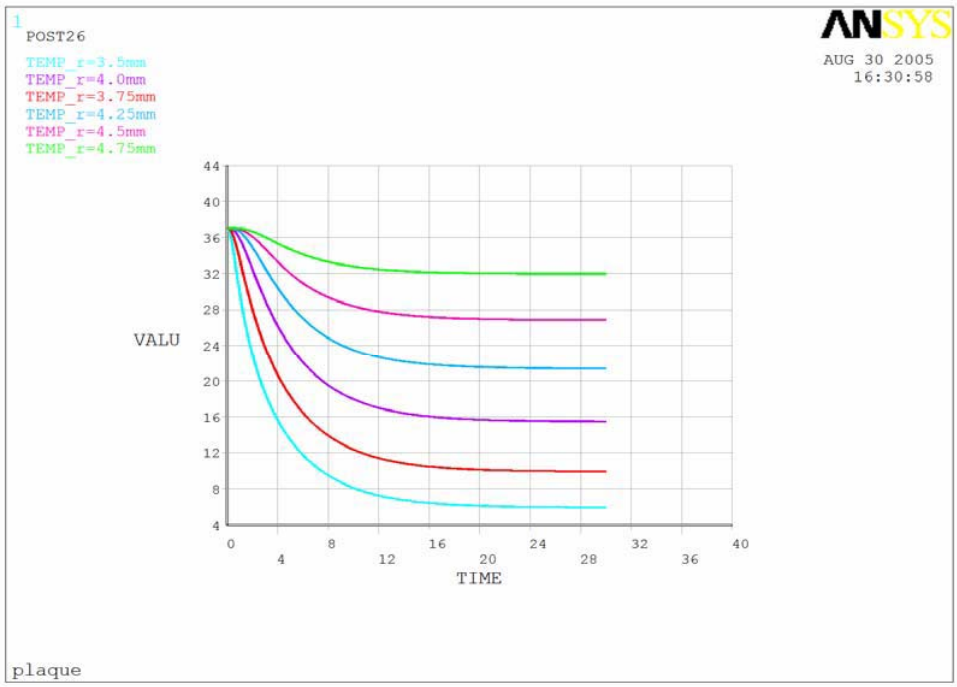

Figure 3.3 Temperature distribution plot of selected nodes located at plaque and arterial wall at -10°C (>60 secs).

3.6 Optimize of Balloon Temperature and Treatment Time

The goal of this section is to find out the durations required to freeze the different thickness of plaques by using different treatment temperature. Investigation of this relationship may somehow help physicians predict the treatment result and come up with a better treatment strategy. Various plaque thickness models are subjected to different treatment temperatures. Optimal treatment is based on following criteria:

1. The inflation of balloon stop once plaque is totally in contact with the balloon surface
2. The treatment is focused on the blockage of lumen excess at least 60% of blockage of lumen
3. The effective freezing temperature is determined as -5°C, which turns gel-like plaque into solid state

The freezing temperature for different plaque thickness and corresponding effective freezing time is plotted in Figure 3.4. As expected, the thicker plaque requires a longer time to complete the ablation. Using lower temperature can essentially reduce the treatment time to induce the same lesion depth.

Furthermore, the effective freezing temperature has to be known to perform cryoplasty to certain range of plaque thickness. For example, in 70% lumen blockage the plaque thickness is about 1.47mm. Using balloon temperature of -95°C, the treatment time was found to be 32.02 seconds. Temperature warmer than -95°C was found to be ineffective to induce the expected lesion depth, even extend the treatment time. This is because the temperature of interface between plaque and arterial wall never reach -5°C, this due to the large effect of the boundary condition of 37°C at the outer boundary of the arterial wall. This

result further concludes that cryoplasty may be unable to completely freeze the plaque region to the desired temperature when a single constant treatment temperature is applied for every patient, since patients have different percentage of blockage. If this is the case, the solidified plaque region maybe first cleaned up by the technique such as atherectomy [30], then undergo a second freezing treatment.

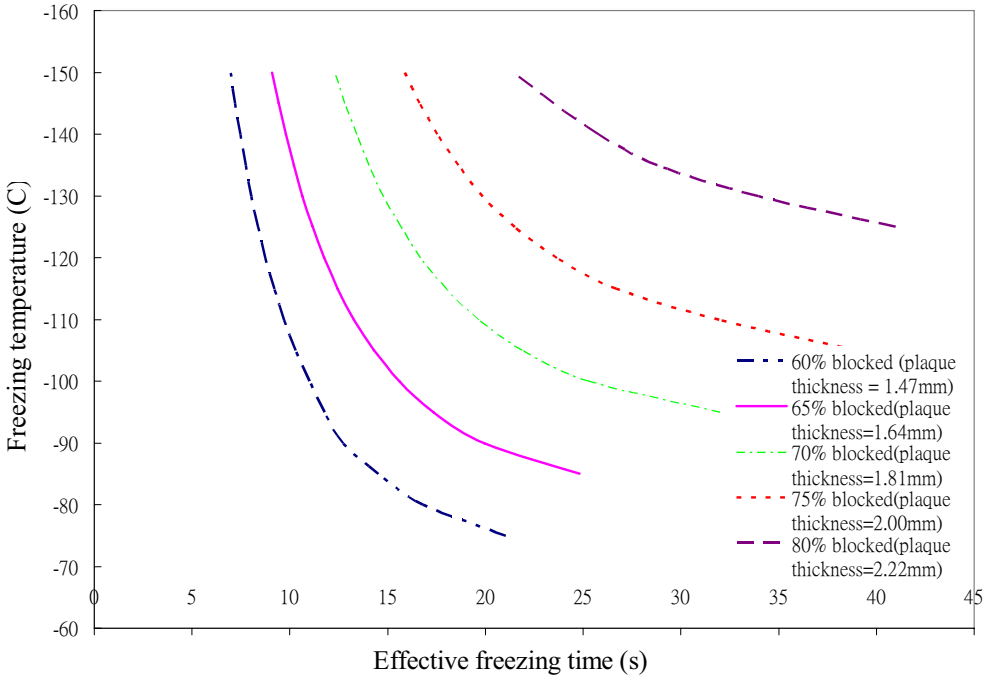

Figure 3.4 Thickness variation of plaque with freezing temperature and time.

3.7 Types of Atherosclerotic Plaque and Its Thermal Characteristics

Different types of atherosclerotic plaques are usually found in the medical investigations. Based on their physical compositions and characteristics, plaques are normally categorized into three types. These are fatty, fibrous, and calcified plaque.

Fatty plaque: fatty plaque contains mostly the fatty streaks and some fibrous elements such as collagen. According to the response to injured hypothesis [7], the first step of atherogensis is the development of fatty streaks, small sub-endothelial deposits of lipid. The exact cause for this process is unknown, and fatty streaks may appear and disappear in sequences, result fatty streaks are not clinically significant. However, they can accumulate smooth muscle cells, migrate from the media and causes the lesions to grow.

Fibrous plaque: fibrous plaque is localized under the intima, within the wall of the artery resulting in the thickening and the expanding of the wall and, sometimes, localized narrowing of the lumen with some atrophies of the muscular layer. The fibrous plaque mainly contains collagen fibres, precipitates of calcium and, rarely, lipid-laden cells [48].

Calcified plaque: the result of an advanced lesion is often characterized by a lipid core that is completely necrotic or necrotic mixed with hemorrhage, separated from the blood flow by a layer of fibrous tissue called the fibrous cap. Intracellular mocrocalcifications form within smooth muscle cells of the surrounding muscular layer, specially the muscle cells adjacent to atheromas. In time, as cells die, this leads to extra cellular calcium deposits between the muscular wall and the outer portion of plaque. In this end stage of atherogenesis, advanced lesion which develops calcifications in the plaque has been called calcified plaque.

In different parts of the body, certain predominant types of plaques are most likely to

be deposited on the linings of the blood vessel wall. For example, calcified plaques are more commonly found in the blood vessels of the leg and limbs whereas fatty and fibrous-fatty plaques are usually deposited in the coronary arteries. For the cryoplasty to be performed in different parts of the body to treat different type of plaques, analysis of thermal characteristics of plaques may help in the cryoplasty treatment planning.

Numerical analysis was performed to determine whether certain type of plaques would have a higher thermal sensitivity to cryoplaty ablation. The parameters of thermal physical properties of plaques are based on Valvano et al. measurements [26]. They categorized the plaques by gross visual observation. The calcified plaques were hard and bony. The fibrous plaques were firm but pliable. The fatty plaques were loose and buttery.

75% lumen blocked model with plaque thickness of 2.0 mm was chosen by applying freezing temperature of -120°C for 25 seconds. The temperature history plot of plaque-artery interface for different type of plaque is shown in Figure 3.5. In Figure 3.5, the result showed that the amount of thermal energy absorbed in the plaque varied according to the predominant plaque type in the cryoplasty model. Because of the higher water content, the thermal conductivity and specific heat values for calcified plaque were the highest. Applying an equal amount of freezing temperature for all three cases resulted in higher temperature drops for calcified plaque. Calcified plaque is followed by fatty plaque then fibrous plaque in their ability to absorb thermal energy. The difference between plaque types is 5°C between calcified and fatty at the peak plaque temperature. The difference was much less for fibrous plaque with an approximate 0.8°C difference in comparison to fatty plaque. Another

supported result is shown in Figure 3.6. The temperature of plaque-artery reached -10.4°C in calcified plaque model, whereas, temperature only reached -5.2°C and -4.8°C in fatty plaque model and fibrous model respectively. However, in medical observation, plaques normally consist of a mixture of various plaque types. Therefore, for thermal analysis, it is reasonable to average all three types of plaques thermal properties for temperature calculating, despite using only one of them alone.

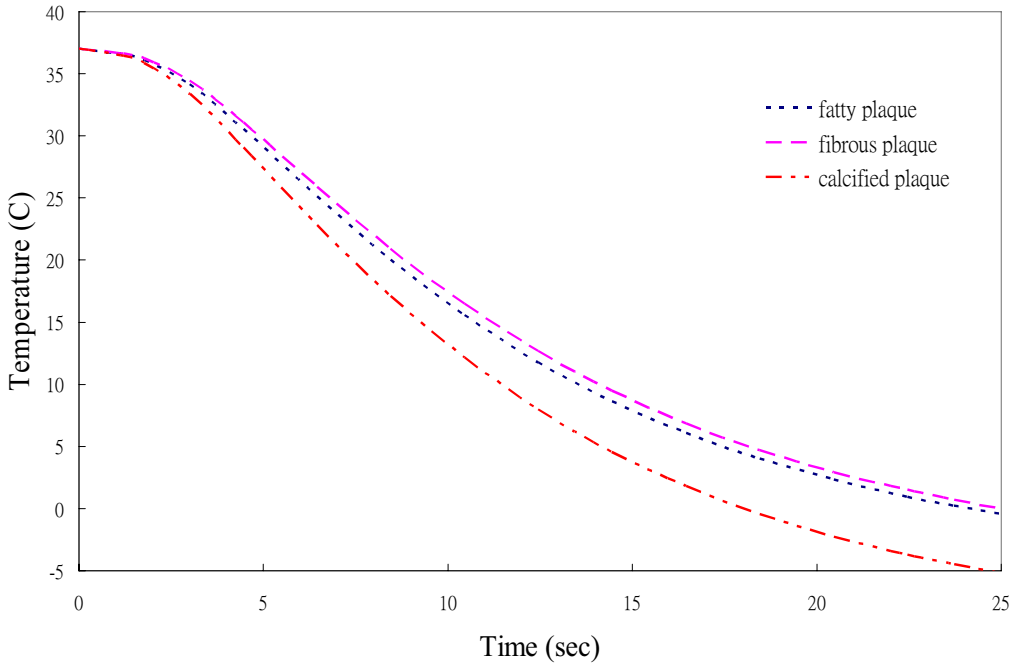

Figure 3.5 Temperature history plots of plaque-artery interface for different plaque models.

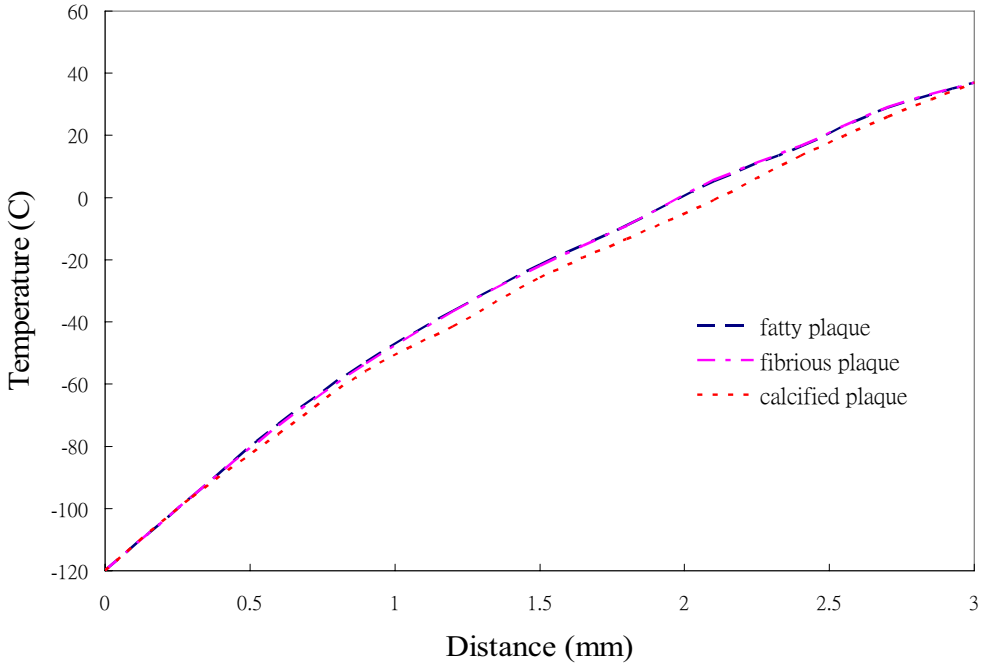

Figure 3.6 Temperature distributions plot as a function of different type of plaques in cryoplaty ablation.

3.8 Sensitivity Test

Parameter sensitivity test was performed to find out the factors which may affect the temperature changes within the tissue during the cryoplasty ablation procedure. Assume that the physical thermal properties such as thermal conductivity, heat capacity, and density of the arterial wall will not vary from person to person. Similarly, the heat capacity and density of blood will be fairly constant between individuals. The main variant between individuals is the thickness of the arterial wall as well as the blood perfusion rate and the tissue metabolic heat generation may also vary from person to person. To investigate these parameters on the model predictions, a parameter sensitivity study was performed against second and third term of Pennes bio-heat equation. That's recall the bio-heat equation:

$$\rho_t c_t \frac{\partial T}{\partial t} = k_t \frac{1}{r}\frac{\partial}{\partial r}\left(r \frac{\partial T}{\partial r}\right) + \rho_b c_b \omega_b (T_b - T) + q_m \tag{3.5}$$

To examine the contribution of the three terms on the right hand side of equation (4.5), the equation can be normalized the dependent and independent variables in the form:

$$\frac{\rho_t c_t}{t_f}\frac{\partial \theta}{\partial \tau} = \frac{k_t}{R^2}\frac{\partial^2 \theta}{\partial \chi} - \omega_b \rho_b c_b \theta + \frac{q_m}{(T_s - T_b)} \tag{3.6}$$

where $\theta = (T - T_b) / (T_s - T_b)$, $\tau = t / t_f$, where t_f is the freezing or treatment time (s), and $\chi = r/R$, where R is the thickness of arterial wall (mm).

Equation (3.6) suggests that the blood perfusion may contribute to temperature changes in the tissue. The temperature gradient is expected to be steep with larger blood perfusion rate, whereas, the heat generation by the tissue has the minimum effect.

Unfortunately, ANSYS software is impossible to capture the blood perfusion term in Pennes equation. A finite element modeling partial differential equation solver call

FEMLAB® was used. FEMLAB is a modulus add-on the Matlab which can solve partial differential equation in finite element domains. A comparison was made of ANSYS and FEMLAB solution without perfusion term. The model presents 70% of lumen blockage which has plaque thickness of 0.0018 mm subjected to -100°C freezing temperature for 25 seconds. It was shown that there was no significant difference between the ANSYS and FEMLAB solution.

3.8.1 Effect of Metabolism Heat Generation

Metabolism is the chemical reaction inside individual cells that produce energy to perform bodily activities and to build new structure. Heat is continuously generated by cells when nutrient is consumed. To investigate whether the metabolic heat generated by tissue will affect the temperature profile during therapy or not, three different value of rate of metabolic heat generation are assumed: 0, 140, 5540 w/m^{-3} and applied into the model. The temperature profile of arterial wall cooled by using temperature -120°C for 30 seconds with three different metabolic heat generation is illustrated in Figure 3.7. In Figure 3.7, temperature profiles for three cases are imperceptible as temperature curves almost overlap each other. Therefore, it is reasonable to neglect the metabolic heat term from the model since its effect is negligible.

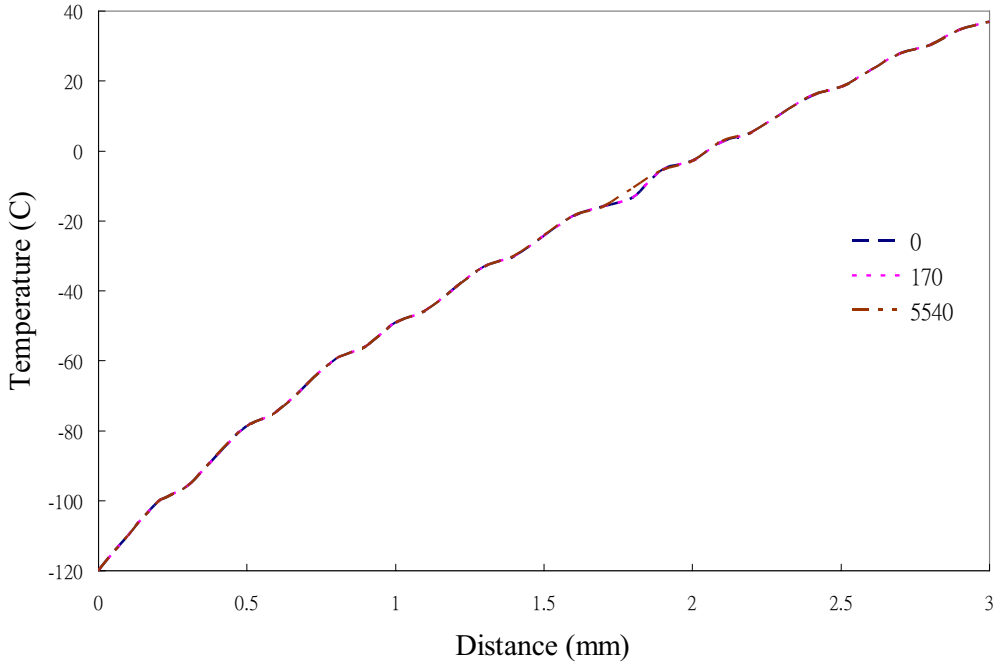

Figure 3.7 Arterial wall temperature profile at temperature of -120°C for different metabolic rates (Q_m: 0, 140, 5540 w/m^{-3}).

3.8.2 Effect of Blood Perfusion Rate

The blood perfusion rate of $0.0028\, m_b^3 m_t^{-3} s^{-1}$ of human muscle has been reported [31]. Assume that the smooth muscle tissue has the similar blood perfusion rate of muscle. A range of blood perfusion rate ω_b: 0, 0.0014, 0.0028, 0.0056 $m_b^3 m_t^{-3} s^{-1}$ are selected to investigate the effect of temperature changes in the tissue during freezing. The results of model simulations for these four cases are presented in Figure 3.8.

As expected, the temperature profiles are steeper at the higher blood perfusion rates. In the regions where the blood perfusion rate is zero, the temperature profile is almost linear. As seen in Figure 3.8, at distance 2mm from arterial wall inner surface, where the blood perfusion rate is zero, the interface between plaque and arterial wall reach the effective temperature -5°C. At the same distance for the blood perfusion is $0.0056\, m_b^3 m_t^{-3} s^{-1}$, the interface temperature reached only 2°C, this is due to the arterial tissue continuously being protected by the blood perfusion from temperature decreases. The freezing temperature from the balloon was essentially withdrawn by the blood, which has a temperature 37°C flows through the capillaries across the arterial wall.

The blood perfusion effect of temperature distribution during the cyoplaty ablation was simulated in FEMLAB. The temperature distribution contour plot with no blood perfusion was shown in Figure 3.9 compare with blood perfusion rate of $0.0056\, m_b^3 m_t^{-3} s^{-1}$ in Figure 3.10. As the figures shown, the arterial wall tissue near the plaque-artery interface already experienced the temperature at -12°C by applying freezing temperature of -120°C for 30 seconds. Meanwhile, for blood perfusion rate of $0.0056\, m_b^3 m_t^{-3} s^{-1}$ in Figure 3.10, the arterial tissue still remained at 37°C. Significant blood perfusion effect showed that the propagation

of freezing front was slowing down while the freezing temperature was continually removed by the blood flowing through the small blood vessel in the arterial wall.

A study of microwave angioplasty showed the similar thermal analysis results when the blood perfusion term in the bio-heat equation was accounted [49]. Higher blood perfusion rate caused the heat to dissipate at a faster rate in the blood vessel wall. Despite, microwave angioplasty technique using high temperature to melt the plaque, the results showed that the blood perfusion has significant effect of temperature distribution during the thermal ablation performed inside the blood vessel.

When the blood perfusion rate was assigned into the model, the model showed very sensitive to this value, this was probably due to the small scale of the control volume of our model. However, in cryoplasty ablation, the blood perfusion effect may be different. The arterial tissue blood perfusion rate is expected largely smaller than the muscle tissue, also blood perfusion is not constant during the ablation. During the freezing ablation, blood perfusion to the arterial tissue may change due to decreasing temperature and distension resulting from the pressure in the balloon [32]. Because of these possible effects, it is difficult to determine the exact value of blood perfusion rate during inflation of the balloon. In contrast, the blood perfusion term contributes strongly to the temperature changes in the tissues, increased in blood perfusion rate essentially result in the limitation of tissue to achieve the desired temperature.

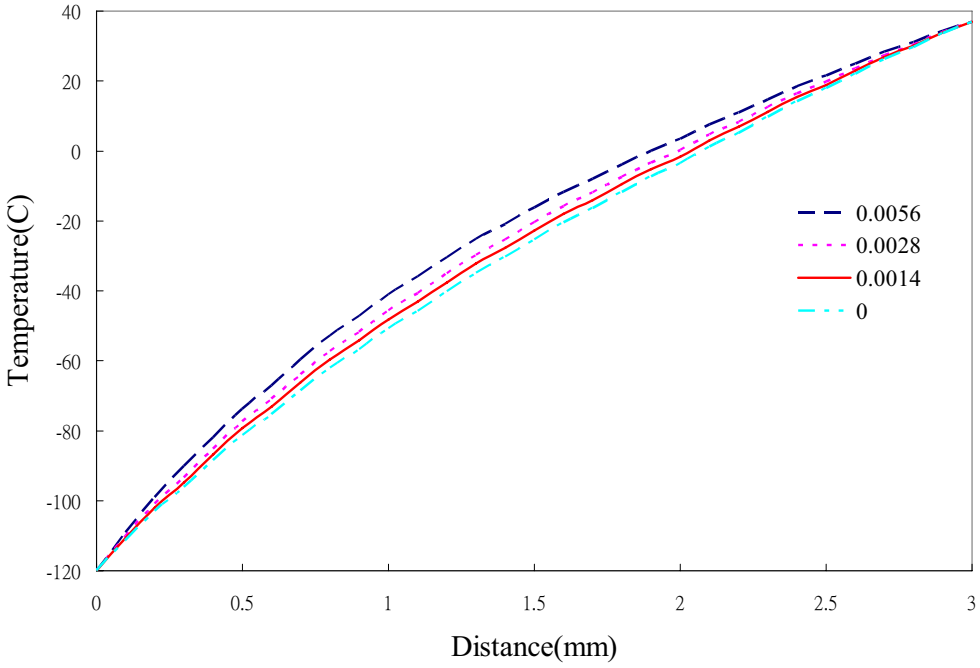

Figure 3.8 Arterial wall temperature profile at temperature of -120°C for different blood perfusion rates (ω_b: 0, 0.0014, 0.0028, 0.0056 $m_b^3 m_t^{-3} s^{-1}$).

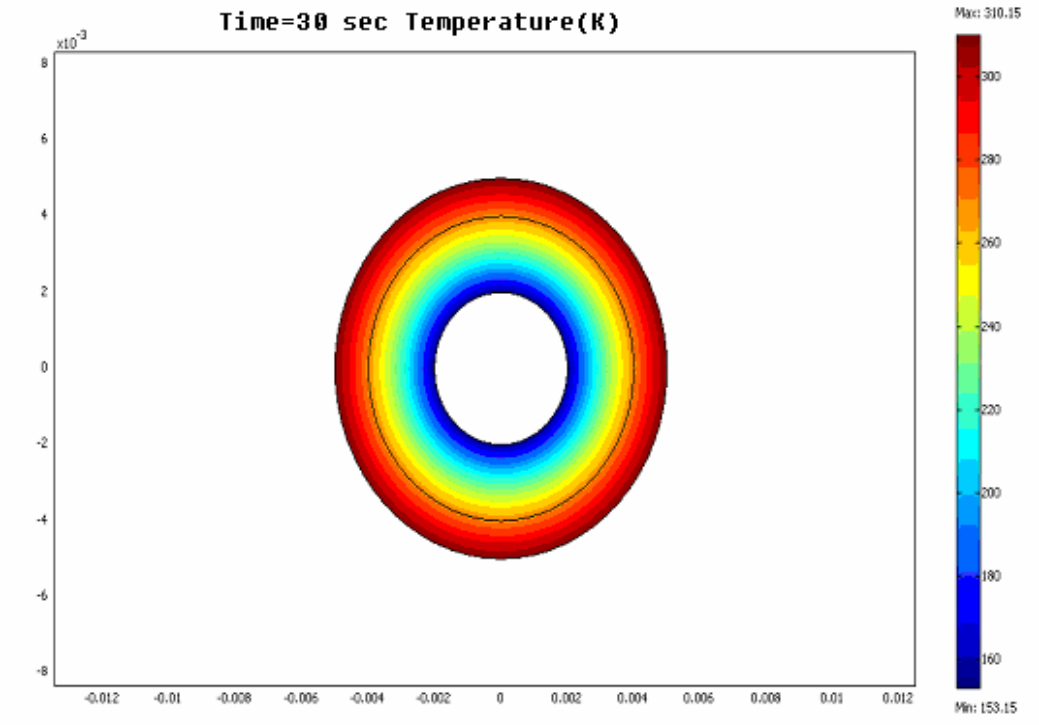

Figure 3.9 Plaque and arterial wall temperature profile at a balloon temperature of -120°C with no blood perfusion effect.

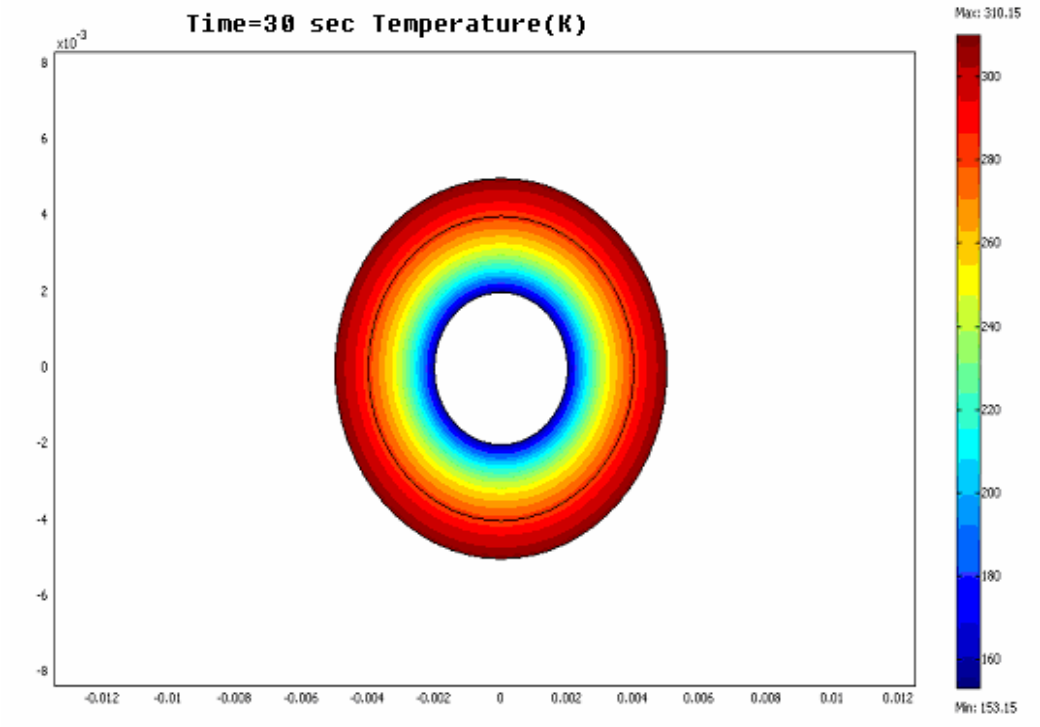

Figure 3.10 Plaque and arterial wall temperature profile at a balloon temperature of -120°C with blood perfusion rate of 0.0056 $m_b^3 m_t^{-3} s^{-1}$.

3.9 Convergence Test

A fundamental premise of using the finite element procedure is that the body is sub-divided up into small discrete regions known as finite elements. These elements are defined by nodes and interpolation functions. Governing equations are written for each element and these elements are assembled into a global matrix. Loads and constraints are applied and the solution is then determined. Convergence test was conducted in ANSYS in order to test the accuracy of the solutions obtained from ANSYS.

Three element size lengths: 0.01, 0.25, 0.5 were selected to perform the convergence tests. The solutions were obtained from the selected nodes within the model control volume. If the results differ by a large amount, however, it will be necessary to try a finer element size. In general, finer mesh returns more accurate solution results we can trust, however, it consumes more computing time and more computer memory is required due to smaller size elements used and result in increase the number of elements.

The convergence tests performed in ANSYS used element size length equal 0.01, 0.25, and 0.5. The results of convergence tests for three different element sizes are shown in Figure 3.11, Figure 3.12, and Figure 3.13. No significant differences were observed in these temperature solutions results. The temperature solutions did not change while reducing the element size and defining finer mesh in the model control volume. The only difference during the tests was the computing time required. Time required to obtain the solutions in element size equal 0.5 model was about 30 seconds, whereas in 0.25 and 0.01 model were 180 seconds and 4.5 minutes respectively. The results indicated that the use of element size of 0.5 was fair enough to obtain accurate solution domains in our thermal finite element model

while minimizing the computer calculating time.

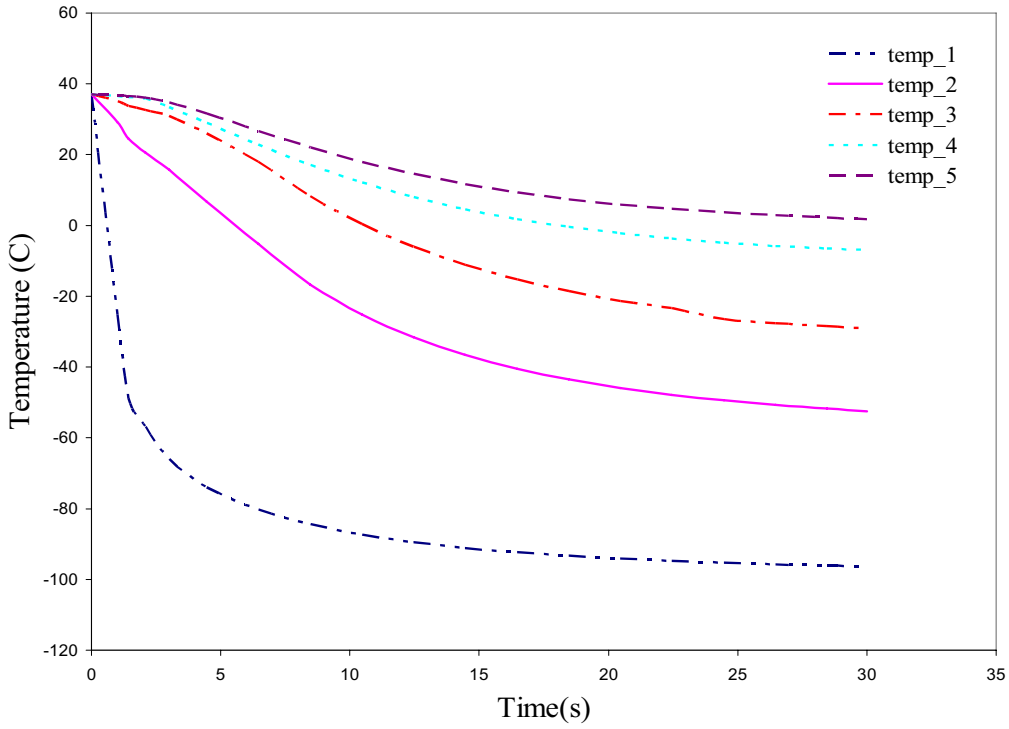

Figure 3.11 Temperatures at select nodes for element size length equal to 0.5 in convergence test.

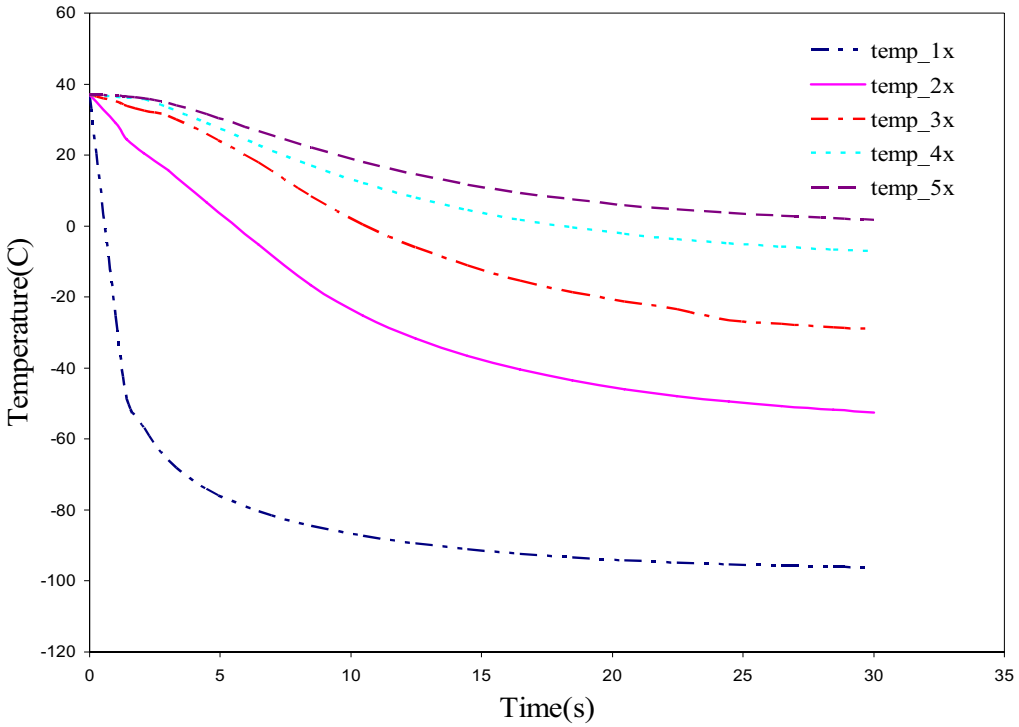

Figure 3.12 Temperatures at select nodes for element size length equal 0.25 in convergence test.

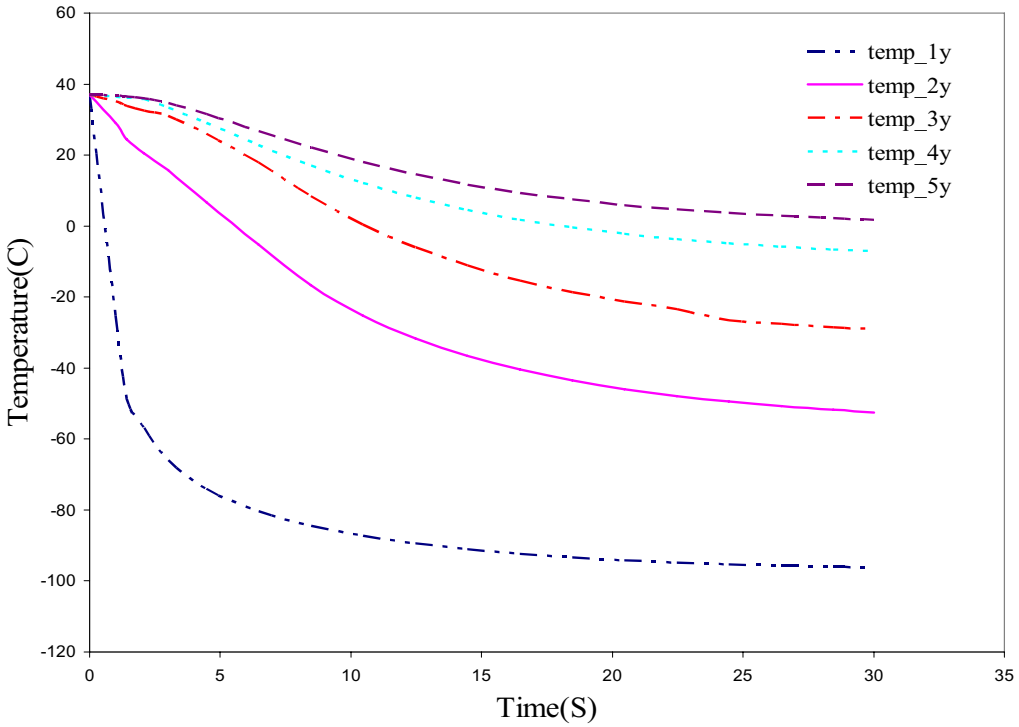

Figure 3.13 Temperatures at select nodes for element size length equal 0.01 in convergence test.

CHAPTER 4

MASS TRANSFER IN THE ARTERIAL WALL

Numerical modeling of mass transport of molecules between blood and artery wall has been widely applied to study the process of atherosclerosis and localize the disease region. It is believed that mass transfer between the blood and the artery wall must play some role in the development of atherosclerosis. The significant evidence comes from the accumulation of high molecular weight lipoproteins within the arterial wall in the early stage of atherosclerosis [31].

A diffusion model of arterial wall was developed in ANSYS to study the mass transfer in the arterial wall. More precisely, the model was used to study the pressure effects on low-density lipoprotein particles uptake in arterial wall. Previous studies in vivo and in vitro have shown that pressure resulted from hemodynamic factors has significant effects on particles deposition in the arterial wall [39-41, 60]. The model was also used to predict concentration distribution of LDL accumulate into arterial wall as function of arterial wall permeability.

4.1 Role of Low Density Lipoprotein in Atherogenesis

Researchers have studied the exchange of substances between blood and the arterial wall. It was believed that abnormal mass transport between the blood and artery wall must play some important roles in the development of atherosclerosis. Substances of interest include oxygen, low density lipoprotein, and platelet-derived cytokines. Among these, low density lipoprotein attracts the most concern, it is because high concentration of low density

lipoprotein in the blood often considered the most important risk factor linked to atherosclerosis and excess low density lipoprotein (LDL) particles accumulate in the intima was believed to trigger the main event in atherogenesis [34, 50, 51], however, not directly proven yet. A great review of role of low density lipoprotein in atherogenesis and development of arterial disease was done by Grundy et al. [52].

Low density lipoprotein (LDL) is a plasma lipoprotein particle whose lipid component includes cholesterol and triglycerides and is commonly referred to as bad cholesterol. LDL particles are responsible for transporting triglyceride fatty acids from the liver to peripheral tissues for utilization [38]. About 75% of LDL is removed from circulation by the LDL receptor when it goes back to the liver, with the remainder going to other tissues.

Based on researchers' findings and several hypotheses of atherogensis, LDL involved in the developing of atherosclerotic plaque can be summarized below:

(1) Endothelial-injury theory reveals that the first step in atherogenesis is entdothelial damage [7]. According to this theory, endothelial damage results in platelet aggression on the injured surface which essentially increase the wall surface adhesive behavior.

(2) LDL carries cholesterol passes the endothelial cells and penetrates into arterial wall from circulation. The rate of penetration appears to depend on the plasma concentration [7].

(3) When large amount of cholesterol in the intima results in fatty streak appearing in injured site, which is the first visible stage of atherogenesis.

(4) LDL particles uptake by macrophage and become foam cells in fatty streak. Here, another popular theory states that LDL particles within the arterial wall become partially oxidized, which renders them susceptible to macrophage recognition and uptake [9].

(5) As atherosclerotic plaque advances, more and more cholesterol is accumulated in smooth muscle. Smooth muscle cells undergo the similar process and convert into foam cells. Large amount of foam cells in fatty streak finally ends up to form the fibrous plaque.

In the combined above stages of atherogenesis, LDL appears to be necessary for the formation of the fatty streak; and without the formation of this lesion, there will be no progression to fibrous plaque. Furthermore, it has been reported that in populations in which LDL cholesterol concentrations are low, the development of advance atherosclerosis appears to be relatively rare, even when other risk factors (eg., smoking, hypertension, and diabetes mellitus) related to atherosclerosis are frequent [48]. In contrast, LDL must play an important role in the development of atherosclerotic plaque.

4.2 Effects of Pressure on Particle Deposition in Artery

Early accumulation of low density lipoprotein in the endothelial space seems to be required to trigger the atherogensis [31]. Mechanisms of transport and distribution of plasma macromolecules in the arterial wall is strongly correlated with hemodynamic factors [34, 51]. In particular, hypertension is a well known risk factor, especially when associated with hypercholesterolemia [43].

Tedgui et al. investigated the effects of pressure on the low density lipoprotein and albumin transport and distribution across the rabbit arterial wall at both low pressure (70mmHg) and high pressure (160mmHg). Their experiment results showed that artery pressurized at 70mmHg, the relative concentration of albumin was found to be higher than that of LDL. This might be due to higher permeability of artery endothelium to albumin than

LDL. In vivo studies have reported that endothelial permeability to albumin ($0.4x10^{-7}$ cm/sec) was about two times higher than that of LDL ($0.2x10^{-7}$ cm/sec) [60]. When the transmural pressure was increased to 160 mmHg, both albumin and LDL relative concentrations were increased. Tedgui et al. further suggested that LDL was forced by pressure-driven convection into a porous material. Concentration profile of LDL showed that most LDL accumulated at endothelial layer, this is because the media is poorly permeable to the lipoprotein.

However, in an ex vivo study by Chesler et al. presented the different result [61]. They setup an experiment in vitro to test the pressure effects on particle deposition in live procine carotid arteries. They cited two mean pressure levels, 100 and 200 mmHg. Their results showed that surface particle deposition did not significantly change with pressure for either the steady or the pulsatile waveform, under either no-flow or flow conditions. They explained this resulted because permeability of artery may decrease slightly with pressure due to radial tissue compression and compaction, so that increases in transmural fluid flow and thus accumulation of large particles are not significant as pressure increase. Obviously, their results were totally different from Tedgui et al. findings. Tedgui et al. reported the endothelial permeability increased at high pressure of 160 mmHg, the result was due to pressure-induced wall distension.

4.3 Modeling Mass Transfer in ANSYS

4.3.1 Theory

It was assumed that the molecular transport into the arterial wall is governed by the three-dimensional convection-diffusion equation. The three-dimensional convection-diffusion

equation in Cartesian coordinates is:

$$\rho c\left(\frac{\partial T}{\partial t}+V_x\frac{\partial T}{\partial x}+V_y\frac{\partial T}{\partial y}+V_z\frac{\partial T}{\partial z}\right)=k_x\frac{\partial^2 T}{\partial x^2}+k_y\frac{\partial^2 T}{\partial y^2}+k_z\frac{\partial^2 T}{\partial z^2}+\dot{Q} \tag{4.1}$$

In order to model mass transport in ANSYS, a thermal analog which describes the correlation between mass and heat transport in a physical system is used to perform analyses. A correspondence between thermal parameters in equation (4.1) and mass transport parameters is presented in Table 4.1 [36].

Making the appropriate substitutions from the Table 4.1, the governing equation for the mass transfer analysis is:

$$\rho\left(\frac{\partial C}{\partial t}+V_x\frac{\partial C}{\partial x}+V_y\frac{\partial C}{\partial y}+V_z\frac{\partial C}{\partial z}\right)=k_x\frac{\partial^2 C}{\partial x^2}+k_y\frac{\partial^2 C}{\partial y^2}+k_z\frac{\partial^2 C}{\partial z^2}+\dot{M} \tag{4.2}$$

Or in term of diffusivity:

$$\left(\frac{\partial C}{\partial t}+V_x\frac{\partial C}{\partial x}+V_y\frac{\partial C}{\partial y}+V_z\frac{\partial C}{\partial z}\right)=D_x\frac{\partial^2 C}{\partial x^2}+D_y\frac{\partial^2 C}{\partial y^2}+D_z\frac{\partial^2 C}{\partial z^2}+\frac{\dot{M}}{\rho} \tag{4.3}$$

The governing equation is solved by a three-dimensional model in ANSYS. Some appropriate assumptions are made to simplify the problem:

(1) Assume that the specie we are interested in is low density lipoprotein (LDL), main carrier of cholesterol into the intima. Even though, there are other molecules such as leukocytes and smooth muscle cells accumulate in intima.

(2) The diffusion of LDL through the arterial wall is driven by the concentration gradient

(3) Assume that the convection process is associated with the flow of blood in or through the vessel wall. The flow is driven by pressure gradient of the wall.

(4) Assume that the permeability of the arterial wall to LDL molecules is $K = 2\times10^{-4}$ μm/s

(5) Assume that the convection process is dominated by a transmural flow of fluid through

the vessel wall, and the convection velocity is determined by a hydraulic conductance.

TABLE 4.1

THERMAL ANALOG CONVERSION FORMASS TRANSFER MODELING IN ANSYS

[36]

Thermal: Length(m), Mass(kg),Time(s)			Mass: Length(μm), Mass(μg), Time(s)		
Symbol	Description	Units	Symbol	Description	Unit
T	Temperature	K	C	Concentration	μg/μg
α	Thermal diffusivity	M^2/s	D	Particle Diffusivity	$\mu m^2/s$
ρ	Density	kg/m^3	ρ	Density	$\mu g/\mu m^2 s$
c	Specific heat coefficient	J/kgK	c	Mass of particle to increase concentration in unit mass of tissue by one unit of concentration	1 Dimensionless
h	Film coefficient	$W/m^2 K$	h	Mass transfer coefficient	$\mu g/um^2 s$
k	Thermal conductivity	W/m K	k	Particle conductivity	μg/μm s
q	Heat	J	m	Particle mass	μg
$\dot{q}$	Heat transfer rate	W(J/s)	$\dot{m}$	Particle transfer rate	μg/s
$\dot{Q}$	Heat generation rate per unit volume	W/m^3	$\dot{M}$	Particle generation rate per unit volume	$\mu g/\mu m^3$ s
V	Convection velocity	m/s	V	Convection velocity	m/s

4.3.2 ANSYS Solution Methodology

When the mass transfer involves the solid body and a flowing fluid, the most elaborate approach to this kind of problem is computational fluid dynamics (CFD). However, CFD is known to be computationally expensive. A possible solution described in a literature [34] is to exclude the flow completely from the computational domain and use convection boundary conditions for the solid model. This method is achieved by either applying a constant concentration or constant flux on the inner side of the arterial wall. This method has been greatly applied in modeling drug delivery from stent for treating atherosclerosis [36].

A drawback of this method is the greatly increase in the number of elements needed to perform a physically valid simulation, because the accuracy of the solution when employing upwind finite element schemes depends on the element size. In ANSYS, the element size is calculated based on the Peclet number.

$$Pe = \frac{v \cdot L \cdot c}{2k} \tag{4.4}$$

Where v is fluid velocity, L is the element length, c is the specific heat of the fluid, and k is the thermal conductivity of the fluid.

To ensure correct simulation results, Peclet must be less than 1 [35]. Therefore, by increasing fluid speed, the element size has to be decreased. This results in a large number of elements and therefore requires longer computational time.

In ANSYS, to activate the mass transport function, the key is selecting the proper element to generate the model. There is only one element type available with this function in ANSYS, which is SOLID70.

There are five stages in the ANSYS modeling analysis process similar to what we did in

the thermal analysis: construction of the geometrical mode; determination of appropriate material properties; determinations and application of appropriate boundary conditions; solution and post processing.

4.3.3 Geometrical Model

The geometrical model of the arterial wall in this study is presented in Figure 4.1. The model is presented in a 30 degree view of a wall segment. The wall has a thickness of 1 mm with the inner surface area being $1mm^2$. The model consists of 3600 tetrahedral finite elements. The mesh of element size gradually increases from the inner surface of wall toward the outer wall. This is due to the fact that the highest concentration gradient is expected at the inner wall, also the flow velocity is applied on this surface, therefore it must have the smallest mesh schemes.

4.3.4 Material Properties and Other Model Parameters

An isotropic diffusivity of 5 $\mu m^2/s$ was assumed for the LDL through the arterial wall, based on the diffusivity of LDL molecules in blood. [37]. ANSYS calculated diffusivity based on the conductivity, density and specific heat capacity. Density of the wall is 1.06 x 10^{-6} $\mu g/\mu m^3$ [27]. The specific heat capacity was prescribed to unity as shown in Table 2, the conductivity of 5 x 10^{-6} $\mu g/\mu ms$ was specified to produce the appropriate diffusivity. The convection flow is determined by the equation:

$$Vr = L \cdot \Delta p \tag{4.5}$$

where Vr is the velocity component in the radial direction, L is the transmural hydraulic

conductance of vessel wall, $\triangle p$ is the transmural pressure.

4.3.5 Boundary Conditions

Initial conditions for the model are a constant zero concentration of LDL throughout the vessel wall. This implied that plaque is cleaned out after the therapy, and there is no LDL molecules left inside the arterial wall.

The side boundaries (xz and yz planes) are assumed to be adiabatic so molecules diffuse in radial direction only. Similarly the external boundary is treated as adiabatic, implying that there is no concentration gradient across this boundary.

A prescribed concentration or a prescribed input flux must be specified at the boundary at the inlet surface (z=0).

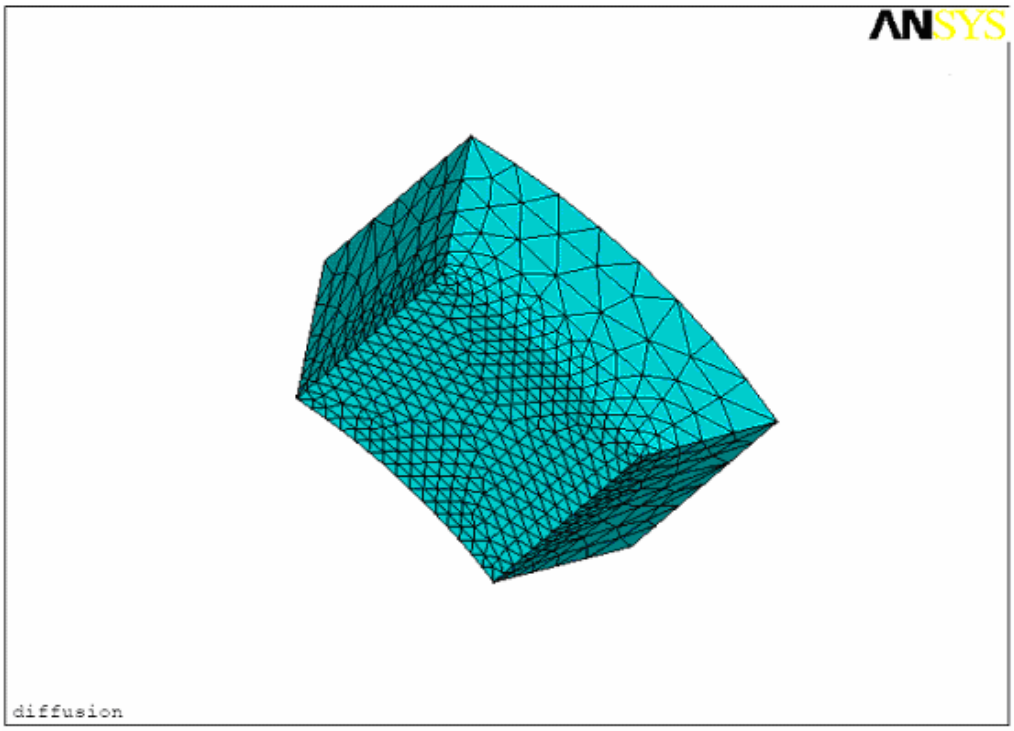

Figure 4.1 Geometrical model of arterial wall in fully meshed used in the mass transfer analysis.

4.3.6 Result

In clinical trial, the risk factor to get atherosclerosis disease is measure the LDL concentration in the blood. It was shown that people has LDL concentration of more than 4.9 mol/L considered very high LDL level and has high risk to get atherosclerosis [38]. Assume that LDL particles flow in the blood stream, initial concentration of LDL at the artery wall surface is 0.049 mol/L.

The transient solution of three-dimensional convection diffusion equation is solved by ANSYS. Time at end of load was set to 800, the time step of 0.01 was used. This returned the distribution of concentration of LDL in arterial at one month is illustrated in Figure 4.2. From the Figure 4.2 to Figure 4.4, we can observe that the transport process of LDL molecules diffuse into arterial wall is very slow. Furthermore, the concentration gradient is not constant along the wall with the highest concentration gradient which was found at the near wall surface area, this indicates that a large amount of LDL molecules were deposited in the endothelial surface area.

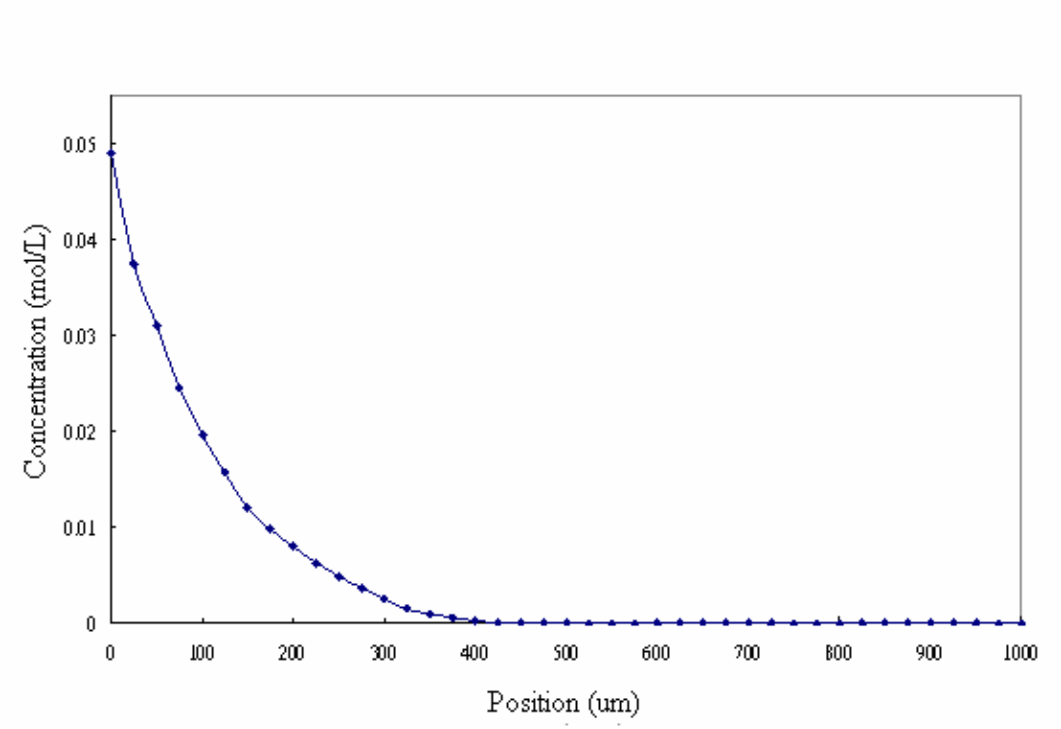

Figure 4.2 LDL concentration distribution within the arterial wall (one month status post-cryoplasty diffusion).

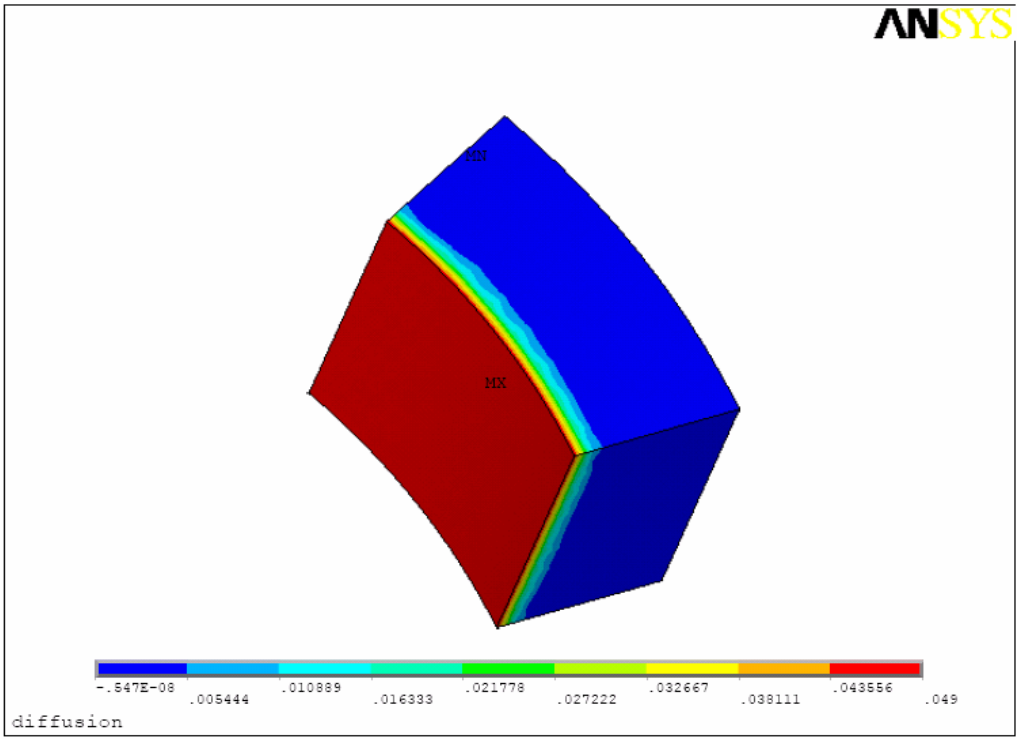

Figure 4.3 LDL contour plot of concentration distribution within the arterial wall (one month status post-cryoplasty diffusion).

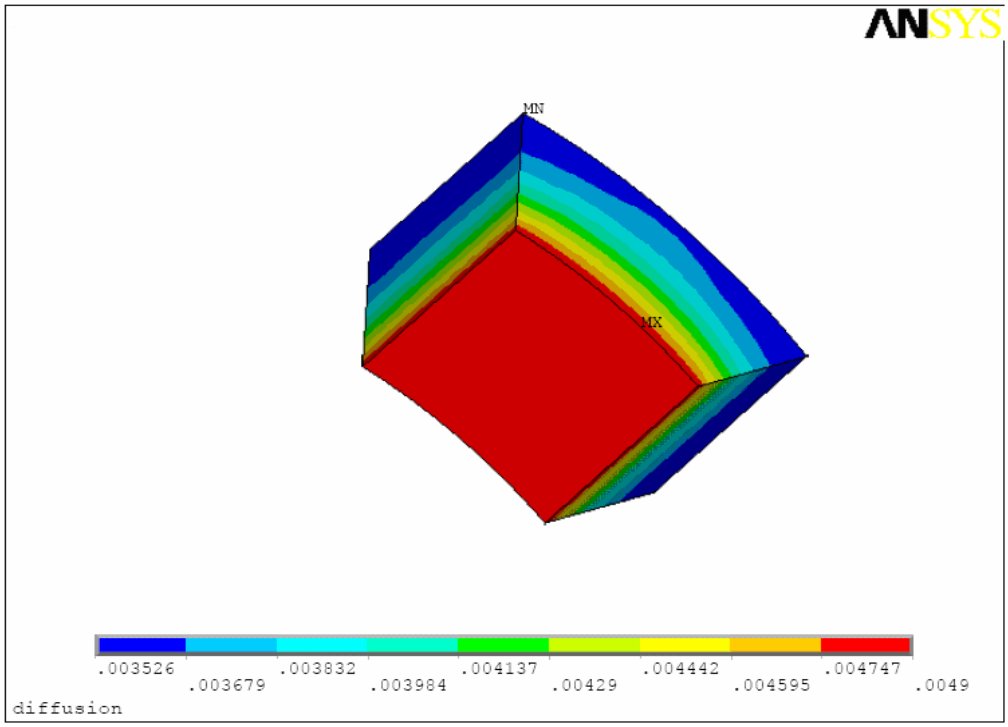

Figure 4.4 LDL contour plot of concentration distribution within the arterial wall (six months status post-cryoplasty diffusion.

4.4 Effect of Transmural Pressure

Fluid dynamic plays important role in molecular transport in the vascular system. An increase in fluid flow, normally known as pressure-driven convection flow or filtration flow, through the arterial wall may enhance molecules diffuse into the wall. Convection fluid flow occurs when there is pressure difference between the inner and outer side of the arterial wall. Previous studies reported that an increase of LDL and albumin transport across the arterial wall as a result of elevated pressure [39-40].

To show the potential effect of pressure, the analysis is repeated by applying different pressure and a hydraulic conductance of 10.19×10^{-4} μm/s/mmHg, based on that measured by Baldwin et al. [41] in a rabbit artery. The convection velocities are calculated by equation (4.5). For three different pressures: 90, 120, and 150 mmHg, the corresponding convection velocities are 0.092, 0.122, 0.153 μm/s respectively. Assume that in cylindrical coordinates, convection flow through an arterial wall occurs in radial direction only, means that the tangential and axis convection velocity components are zero. The results compared with the diffusion only model is shown in Figure 4.5.

As shown in Figure 4.5, the convection mechanism shows influence on the concentration distribution of LDL along the arterial wall. Concentration of LDL molecules are higher in the diffusion and convection model than the diffusion only model, also the concentration of LDL increases with an increase of pressure or the corresponding convection velocity. These results shown agreed with Tedgui et al. findings, elevation of the pressure of the arterial wall may increase the molecules transport into the wall.

In Figure 4.6 and Figure 4.7, the results show that pressure has some influences on the

inlet flux through the arterial wall. For pressure at 150 mmHg, the inlet flux reaches a steady state at 0.12 x 10^{-9} μg/μm^2/s at the fourth month. This result indicates that at a higher pressure, the convection process of plasma flows though the arterial wall faster, thus more LDL particles are expected trapping into arterial wall.

In mass transfer of molecules into the arterial wall, both diffusion and convection are important. When the convection flow is present, convection slightly dominates the transport process. Also, the convection flow is influenced by the pressure. Transmural convective flow is particularly interested in drug delivery into the arterial wall by the drug stent [36] as well as in the research in pathology of atherosclerosis [42].

Moreover, the pressure-driven convection is associated with the arterial hypertension or high blood pressure. A raised in high arterial hypertension can be induced by several factors included: high salt intake, smoking, aging, stress, and high levels of saturated fat in the diet [43]. Nevertheless, in clinical, a high blood pressure or hypertension is often to be believed to be one of risk factors associated to causing strokes, heart attack, heart failure and arterial aneurysm.

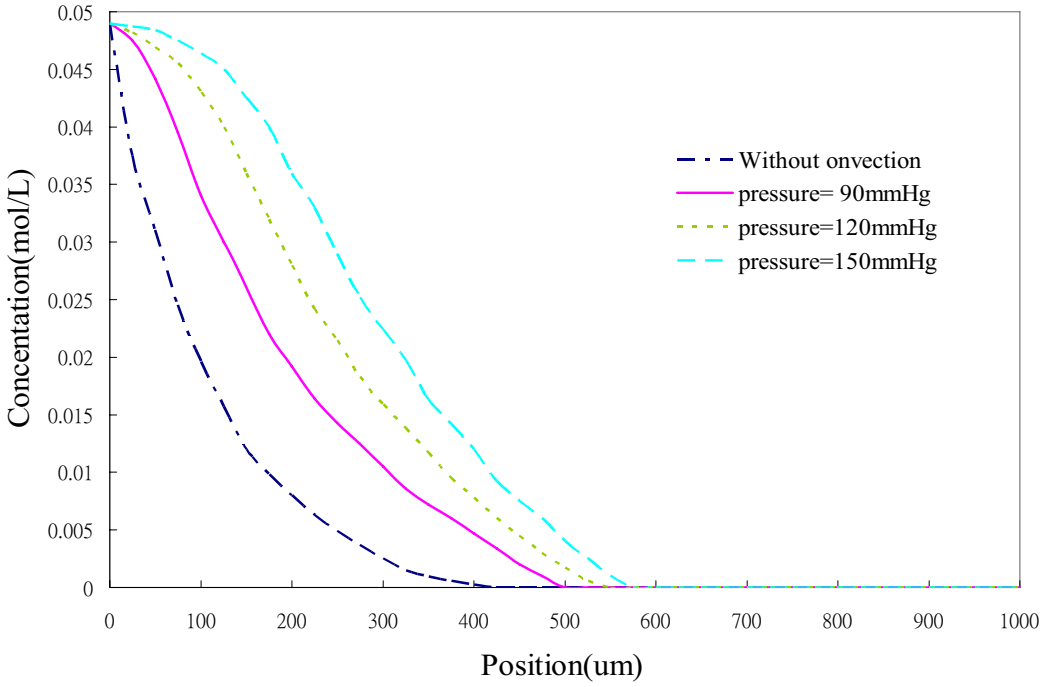

Figure 4.5 Effect of transmural pressure for LDL diffusion in the arterial wall after one month.

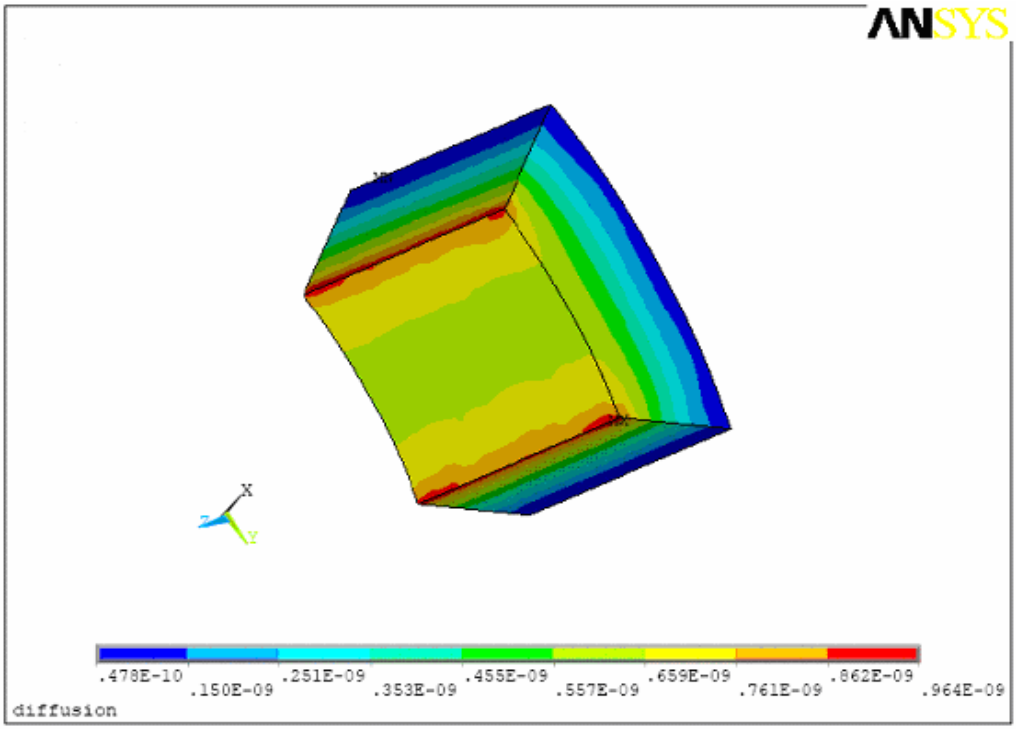

Figure 4.6 Flux through the arterial wall after one month diffusion.

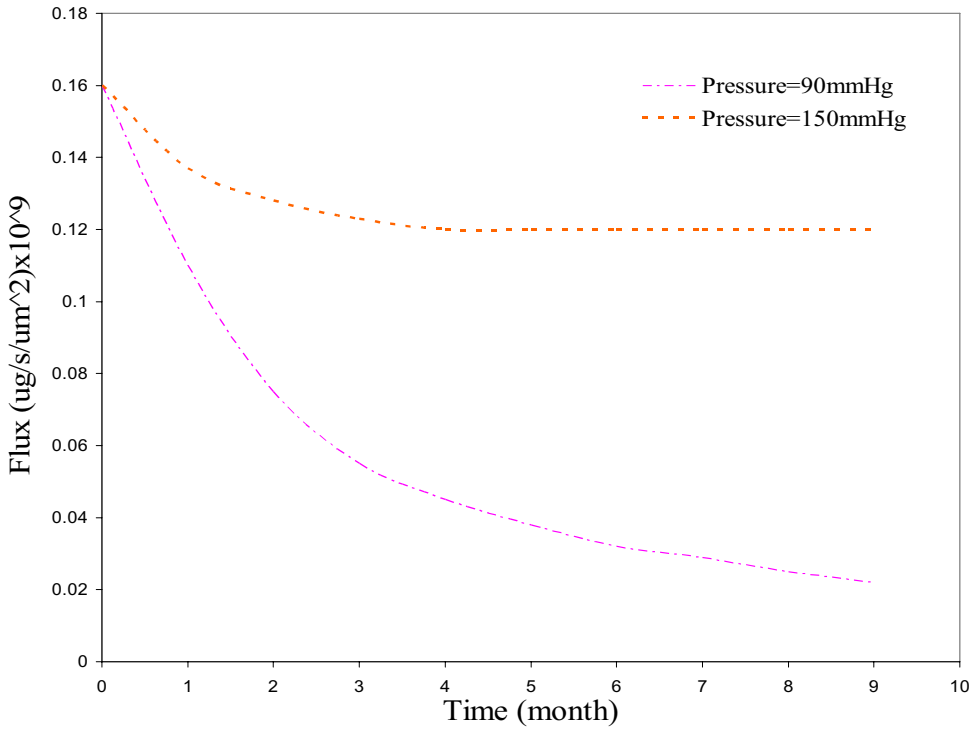

Figure 4.7 Effects of pressure on inlet flux per unit area through arterial wall.

4.5 Effect of Permeability in Molecules Transport

Permeability is one of the most important functions of the endothelial membrane. The endothelial membrane is a thin layer located on the surface of the arterial wall that act as gates that control the mass transfer between the interior and exterior of the wall. Endothelial membranes are selectively permeable. This means only certain molecules are allowed to move in or out of the arterial by diffusion. Assume that the condition of permeability in the arterial membrane change due to wall remodeling after cryotherapy, there must be a change in the diffusion rate of molecules across the membrane as well.

Five different values of arterial wall membrane permeability: $2x10^{-4}$, $4x10^{-4}$, $6x10^{-4}$, $8x10^{-4}$ and $10x10^{-4}$ μm/s are assumed for analysis. The results of the diffusion rate of the corresponding assumed permeability are shown in Figure 4.8. The results illustrate that an increased in the arterial wall permeability results in the increase of the diffusion rate of molecules into the wall. The permeability of the artery is determined by the membrane, only a certain amount and certain type of molecules are allowed to enter the arterial wall. The result shown in Figure 4.8 may be able to explain that when the arterial is injured, large amount of molecules are expected to diffuse into the injured site since the membrane has lost its ability to control diffusion rate.

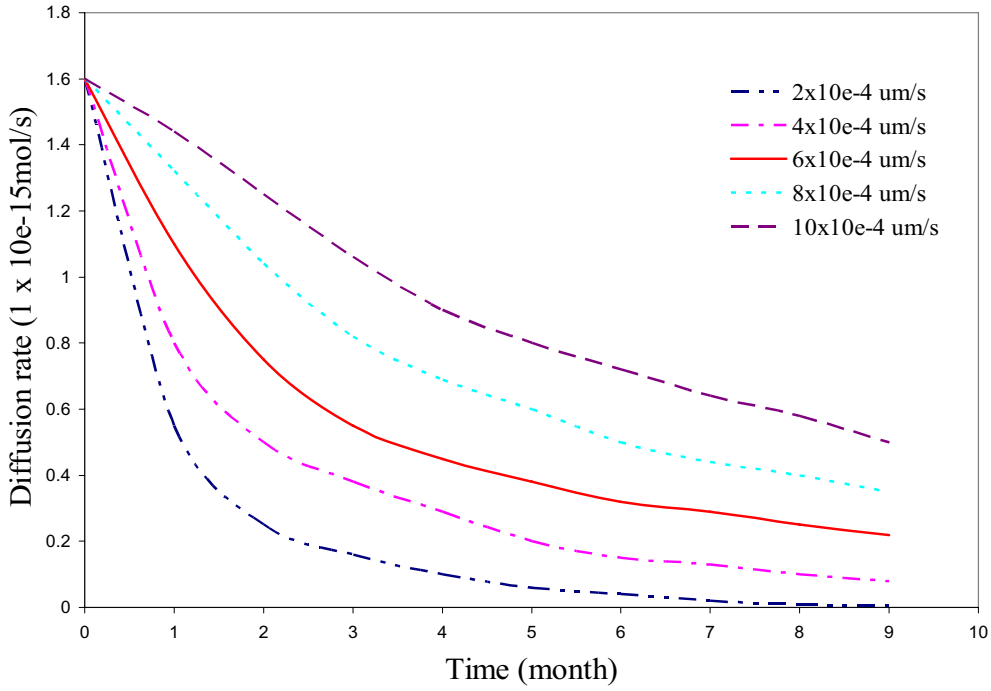

Figure 4.8 LDL Diffusion rate into arterial wall assume different permeability of arterial wall.

CHAPTER 5

REGROWTH OF PLAQUE DURING THE POST-CRYOPLASTY PERIOD

The cryoplasty technique for treating diseased arteries shows potential to delay the period of artery re-clogging and reduce the restenosis rate after angioplasty. However, the exact mechanism induced by cyoplasty to arterial wall tissue and how it prevent restenosis still remain unclear. Study of plaque regowth in post-cryopalsty period become important when the cryopalsty technique may advance to be used in treating atherosclerosis in the carotid artery and coronary artery. Information quantifications are base on the following aspects: (1) comparison of angioplasty and cryoplasty (2) influence of low temperatures to biological tissues (3) effect of blood flow on blood vessel structure after balloon angioplasty.

5.1 A Comparison between Cryoplasty and Angioplasty

Cryoplasty technique is essentially based on angioplasty. Dilation force of the balloon pushes plaque towards the arterial wall to open up the clogged lumen. Despite using the dilation force, there must be other mechanics of cryoplasty to get the different results from angioplasty. Instead of using liquid saline in angioplasty, cryoplasty uses nitrous oxide to optimize the dilation effects of standard angioplasty. James D., a co-inventor of cryoplasty claimed that gas from nitrous oxide causes uniform dilation and minimizes the arterial wall injury, thus preventing the artery from recoiling [53]. Study of restenosis also showed that the negative remodeling of arterial wall after angioplasty was due to the dilation force induced by angioplasty causing excess injury to the arterial wall [11].

Despite nitrous oxide ability to minimize the arterial wall injury, cold thermal energy

transferred to plaque and arterial wall should be the most important factor by using this technique. Smooth muscle cell proliferation is the most serious problem after angioplasty, also it is believed that smooth muscle cells play an important role in restenosis [11]. Smooth muscle cells experience freezing in low temperatures between -5°C to -15°C which results in a process called apoptosis, known as a natural biologic mechanism that results in the removal of unwanted tissue via programmed cell death [3]. Apparently, some smooth muscle cells die by this mechanism, which may postpone the time of restenosis. However, it seems like the effect is not permanent, since proliferation is observed after a period of time [44].

5.2 Influence of Low Temperature on Biological Tissues

Temperatures below physiological temperature of warm blooded organisms, from about 36°C to -40°C are important to biological tissue. It is because temperatures in this range can be either used to preserve biological tissues and cells or destroy undesirable tissue. For example, the cryopreservation technique is used to freeze the cell and store it in a temperature where all metabolic processes are all arrested. The frozen cell can be thawed to fertilize and can be used in future clinical research [54]. In the other hand, the cryosurgery is used to remove and destroy the undesired cancer tumor [55], as well as the recently cryoplasty technique being proposed for treating the diseased artery [3, 16, 17, 18, 44].

An important change in biological systems during freezing should be the cell membrane. The cell membrane is important for the cell which isolates the interior of the cell and sub-cellular components from its exterior. Cell membrane also acts as a gate that controls the interaction and mass transfer between the interior and exterior of the cell. During the freezing,

changes occur in the cell membrane structure and function [56]. The membrane lipids undergo phase transition as the cell experience cooling. The new lipids configuration fails to anchor the membrane proteins tightly and a new opened path forms in the cell membrane, this result the cell membrane looses the ability to isolate the cells interior from its exterior. Furthermore, uncontrolled mass transfer begins to occur between the cell interior and exterior, which leads to cell damage [57].

Another key factor that resulted in the cell damaging by freezing depends on the cooling rate. At a slow cooling rate, cells try to remain equilibrium with the external solution. The external solution freezes before the intracellular medium because of the protective effects of the cell membrane. Thus, the outside of the cell becomes more hypertonic and water flows from the inside to the outside. Removing too much water leads to the death of the cell. At a fast cooling rate, there is less time for water to move out from the cell, which becomes supercooled and eventually intracellular ice forms that is inevitably lethal [54]. In contrast, at a slow cooling rate, cell death is due to long period of exposure to hypertonic conditions; at a fast cooling rate, cell death is associated with intracellular ice formation. An optimum rate of cooling by balancing these two phenomena may results an increase of cell survival rate [58].

5.3 Modeling Plaque Regrowth Based on Biofilm Model

Plaque re-growth on the diseased arterial wall is the major problem which limits the current available techniques for treating atherosclerosis. Restenosis or plaque re-growth occurs in 20-50% of patients after balloon angioplasty and in 10-30% of patients receiving a stent [2]. Even in the most recently proposed technique, cryoplasty, 17% of patients were

found where retenosis occurred at the diseased site after 12 months of receiving treatment [3].

Retensosis involves complex processes which include proliferation of smooth muscle cells inside the internal elastic lamina and migration of smooth muscle cells into the intima and accumulation of macromolecules in the intima again [11].

In this section, biofilm growth model was quantified and applied to model the plaque re-growth in diseased artery. To the best of the author's knowledge, no particular model such as the biofilm growth model has been used for atherosclerotic plaque. This is the first attempt to model plaque re-growth based on biofilm model.

5.3.1 Biofilm Model and Capability

Biofilms are communities of bacteria that attach to surfaces and form heterogeneous three-dimensional structures [62]. Most often, biofilms are unwanted and related to diverse problems as microbial induced corrosion of oil rigs and pipelines [63], food and drinking water contamination [64], dental caries and periodontal diseases and a variety of biomaterial-centered infection in man [65].

The formation of a biofilm can be summarized in the following sequences [66]:

1. When organic matter is present, a conditioning film of adsorbed components is formed on the surface prior to the arrival of the first organisms
2. Microorganisms are transported to the surface through diffusion, convection, sedimentation or active movement
3. Initial microbial adhesion occurs
4. Attachment of adhering microorganisms is strengthened though exopolymer

production and unfolding of cell surface structures

5. Surface growth of attached microorganisms and continued secretion of exopolymers
6. Localized detachment of biofilm organisms caused by occasionally higher fluid shear or other detachment forces operative

From above sequences of biofilm growth, the mechanisms of biofilm formation are very similar to plague buildups. Even though the processes of plaque buildups may be more complex than biofilm, since the events include the inflammation of smooth muscle cells and migration of smooth muscle cell from media to intima. Even more complicated event such as LDL particle being oxidized and transformed into a macrophage. However, the biofilm growth model provides the basic rules and steps of how the plaque grows on the diseased arterial wall.

The schematic of steps in plaque formation is presented in Figure 5.1. The growth of plaque is modeled in the following steps:

1. Injured of endothelial surface due to hypertension or other factors resulted in increase of arterial wall permeability.
2. Particles enter the endothelial surface either by diffusion or convection process.
3. Large amount of particles accumulated in arterial wall surface and activate the growth of atherosclerotic plaque.

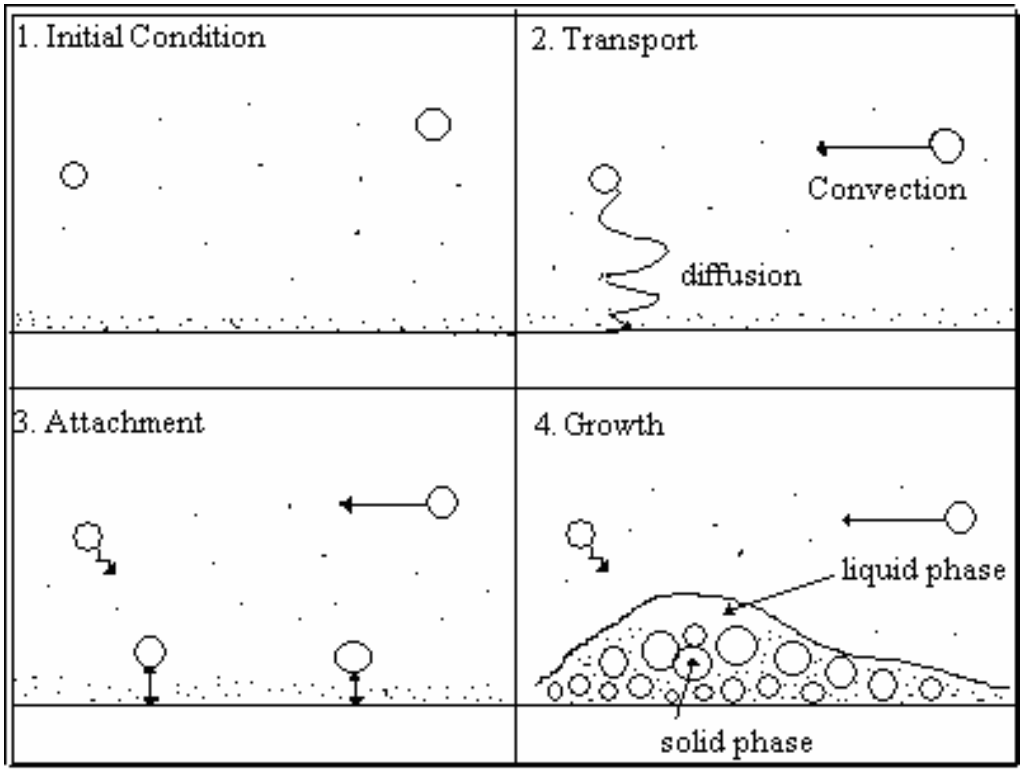

Figure 5.1 Schematic of the steps in plaque formation

5.3.2 Plaque Growth Model

The biofilm model applied in this modeling is based on the multi-species biofilm model given by Wanner et al. [67]. The model is a one dimensional model in space with biofilm growth only normal to the substratum. A biofilm consists of different compartments including the substratum, the biofilm and water. To simplify the problem, assume that only one liquid phase and one solid phase in this modeling. The total plaque region is given by:

$$e_l + e_s = 1 \tag{5.1}$$

where e_l and e_s are fractions of liquid phase and solid phase in total plaque volume.

Liquid Phase:

The mass balance of molecular particles in liquid phase is given by

$$\frac{\partial e_l C_{l,i}}{\partial t} = -\nabla \cdot J_{l,i} + r_{l,i} \qquad i = 1,\ldots\ldots\ldots,\mathrm{N} \tag{5.2}$$

where $C_{l,i}$ $r_{l,i}$ are the concentration and the production rate of the dissolved particles i in liquid phase l.

The flux $J_{l,i}$ of particles in the plaque, due to diffusion, is assumed by Fick's first law as

$$J_{l,i} = -D_{l,i}(X)\nabla C_{l,i} \tag{5.3}$$

where $Dl_{,i}$ ie the diffusion coefficient of dissolved particles i in the plaque. Substitute (5.3) to (5.2) gives

$$\frac{\partial e_l C_{l,i}}{\partial t} = -\nabla \cdot \left(D_{l,i}(X)\nabla C_{l,i}\right) + r_{l,i} \tag{5.4}$$

Solid Phase:

Under the same assumptions, the mass balance for the solid phase in the plaque is given by

$$\frac{\partial e_s \rho_s}{\partial t} = -\nabla \cdot J_s + r_s \tag{5.5}$$

where ρ_s is the density of solid phase, r_s is the production rate of the solid cells, and J_s is the flux of the solid components within the solid phase. The main assumption behind this is the solid plaque phase is mainly subject to a common advection process [68], means that if one particle moves, it causes displacement of its neighboring particles. The J_s will be the an advection flux and is given by

$$J_s = v_s \rho_s e_s \tag{5.6}$$

where $v_s = v_s(X,t)$ is the velocity vector of the solid phase in plaque.

Assume that the plaque growth is predominated normal to the endothelial surface only, it implies that

$$\nabla \cdot J_s = \frac{\partial J_s}{\partial \eta} = \frac{\partial}{\partial \eta}\left(v_s \rho_s e_s\right) \tag{5.7}$$

where η is defined as the direction perpendicular to the endothelial surface, substitute (5.7) into (5.5) gives

$$\frac{\partial e_s \rho_s}{\partial t} = -\frac{\partial}{\partial \eta}\left(v_s \rho_s e_s\right) + r_s \tag{5.8}$$

Assume constant density ρ_s and volume fraction e_s so equation (5.8) simplifies to

$$\frac{\partial v_s}{\partial \eta} = \frac{r_s}{e_s \rho_s} \tag{5.9}$$

Integrating from 0 to η , with boundary condition that the plaque growth velocity v_s at the endothelial surface is zero, then we obtain

$$v_s = \frac{1}{e_s \rho_s} \int_0^{\eta} r_s d\eta \tag{5.10}$$

Let $L_p = L_p(\xi,t)$ be the height of plaque growth at the space point ξ and time t. Assume

that at each point ξ along the surface, the interface is moving at the velocity V_I, normal in the endothelial surface. Then, the movement of the interface is due to the effect of the plaque growth in term of v_s, which gives

$$V_I e_s \rho_s = v_s(L_p) e_s \rho_s \tag{5.11}$$

Furthermore, V_I is related to L_p by

$$V_I = \frac{dL_p(\xi,t)}{dt} \tag{5.12}$$

Combine equation 5.10, 5.11 and 5.12, we obtain the plaque growth equation

$$\frac{dL_p(\xi,t)}{dt} = \frac{1}{e_s \rho_s} \int_0^{L_f(\xi,t)} r_s d\eta \tag{5.13}$$

Since the r_s depends on the $C_{l,i}$, the above equation is coupled with the concentration equation (5.4) in the liquid phase.

Plaque Kinetics

Assume that the plaque growth rate r_s can be modeled by Monod Kinetics [68]

$$r_s = \mu_{\max} \frac{\rho_s C_{l,i}}{K + C_{l,i}} - b\rho_s \tag{5.14}$$

as well as production rate of dissolved particles in liquid phase

$$r_{l,s} = \frac{\mu_{\max}}{Y} \frac{\rho_s C_{l,i}}{K + C_{l,i}} \tag{5.15}$$

5.3.3 Numerical Results

Modeling plaque growth was attempted based on the biofilm growth model. The parameters used in plaque growth simulation are listed in Table 5.1. The simulation result is shown in Figure 5.2. As shown in Figure 5.2, the result shows that plaque grew very fast at

the initial stage then the process slowed down after 15 days. The model result may not fit the real plaque growth well since many real boundary conditions and parameters are unknown. For example, detachment rate is important in the biofilm model, part of the biofilm may be detached from the substratum due to erosion, factors of erosion included nutrient supply, biofilm thickness and hydraulic shear [69]. The problem is that detachment mechanism is unclear in plaque buildup, though we can consider thrombosis or rupture of plaque as detachment. The problem is thrombosis release the particles from plaque into the blood stream, instead of reducing the plaque volume, the plaque expands even larger due to cells migration from the arterial wall. However, without including the detachment term, the process of plaque growth may continue forever, since the plaque will never reach the steady state.

Furthermore, the plaque kinetics is not known, although Monod Kinetics was assumed in this modeling. The Monod kinetics model makes modeling extremely difficult to get realistic result because the Monod saturation coefficient, the endogenous decay coefficient and the yield of cell material, as these terms have to be derived from experimentation. In contrast, biofilm growth model can possibly be applied in plaque growth if the parameters used in simulation can be obtained from experiment approach.

TABLE 5.1

PARAMETERS USED FOR PLAQUE GROWTH MODEL

Parameter	Description	Value	Units
$C_{l,i}$	Initial concentration	100	µg/µm
e_l	Fraction of liquid phase of plaque	0.8	
e_s	Fraction of solid phase of plaque	0.2	
r_s	Growth rate of solid cells	0.8	µg/µm
μ_{max}	Maximum specific growth rate	7.0	1/sec
K	Monod saturation coefficient	1.0	µg/µm
b	Endogenous decay coefficient	1.0	1/sec
Y	The yield of cell material from $C_{l,i}$	0.69	

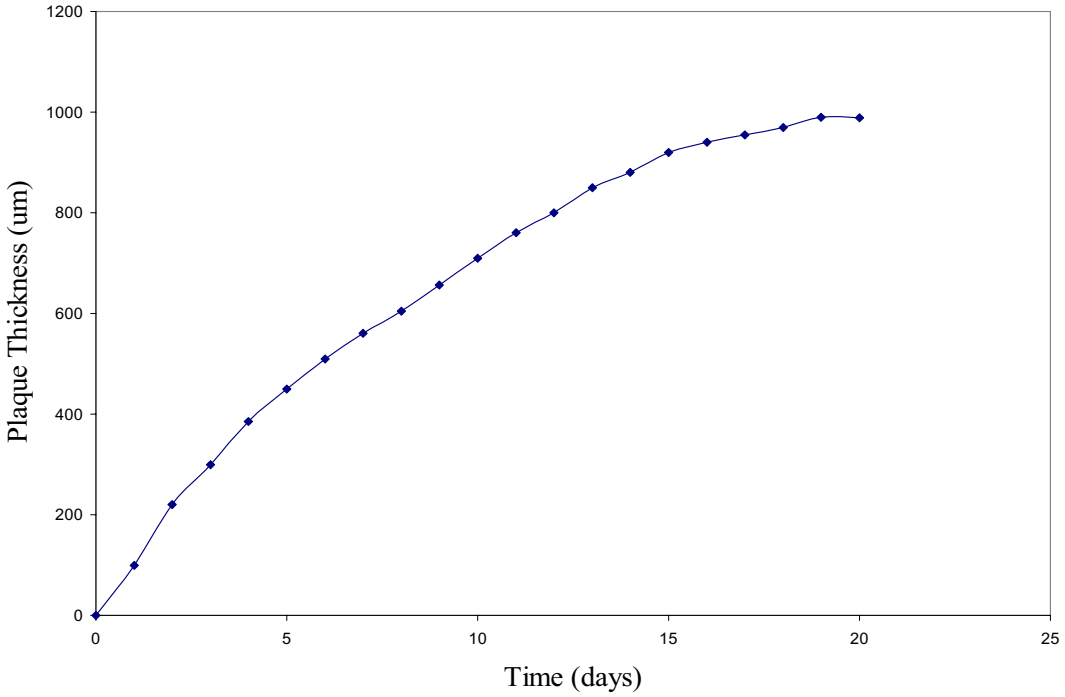

Figure 5.2 Thickness of plaque growth as a function of time

CHAPTER 6

CONCLUSION

Research on cryotherapy ablation has actively been pursued while cryoplasty has shown initial potential to treat atherosclerosis disease by using a controlled freezing method. In this thesis, it has illustrated using element method to study the heat and mass transfer inside the arterial wall and tissue in ANSYS. It was shown that ANSYS is a powerful tool to investigate and answer some phenomena related to medical aspects.

In heat transfer modeling, it was shown that the single treatment temperature of -10°C used in the cryoplasty procedure may not be effective to complete ablation for plaque with different thickness. Lower treatment temperatures as low as -110°C may be required for the patient who has 80% blocked in the lumen. Furthermore, inclusion of the blood perfusion rate results some effects on the temperature distribution change inside the arterial wall during the treatment. Four blood perfusion rates (ω_b: 0, 0.0014, 0.0028, 0.0056 $m_b^3 m_t^{-3} s^{-1}$) were assumed for comparison. It was found that the temperature of the frozen tissue is significantly lower by an increase in blood perfusion. The artery-plaque interface temperature in ω_b = 0.0056 $m_b^3 m_t^{-3} s^{-1}$ case was 7°C higher than the no blood perfusion case after the model was subjected to a freezing temperature -120°C for 30 seconds.

Different types of plaque were also subjected to their thermal characteristics. Applying an equal amount of freezing temperature for all three cases resulted in higher temperature drops for calcified plaque. Calcified plaque is followed by fatty plaque then fibrous plaque in their ability to absorb thermal energy. The difference between plaque types is 5°C between calcified and fatty at the peak plaque temperature. The difference was much less for fibrous

plaque with an approximate 0.8°C difference in comparison to fatty plaque.

In the mass transfer model, the result of modeling showed that both diffusion and convection play important roles in plaque buildup. When the convection flow is present, the diffusion process was slightly dominated by convection. The modeling results also showed that the concentration of LDL along the arterial wall is essentially increased when the wall pressure difference is set to 90, 120, and 150 mmHg respectively, which is consistent with the previous studies. Moreover, the result of convection is due to hypertension of the artery, this can partially explain the person who has high blood pressure may have a higher risk of stroke or heart attack.

Five different values of arterial wall membrane permeability: $2x10^{-4}$, $4x10^{-4}$, $6x10^{-4}$, $8x10^{-4}$ and $10x10^{-4}$ μm/s are assumed for diffusion test. The result of diffusion rate of corresponding assumed permeability illustrated that an increase in the arterial wall permeability results increase the diffusion rate of molecules into the wall. This reveals that permeability change of artery due to injury or other conditions in arterial wall membrane, maybe result in a larger amount of molecules diffusing into the injured site and contributing to plaque buildup due to the membrane loosing its ability to control the mass transfer between arterial wall and blood stream.

The last part of the thesis, demonstrated the plaque growth based on biofilm growth model. The model works well for current problems, except some parameters needed to be determined by experimental method, also some other phenomena need to be added into model such as migration of smooth muscle cells from arterial to plaque.

Future study should focus on measuring proper physical properties of vascular tissue in

low temperature, since tissue is different from other materials because of the presence of a vascular system and its associated blood flow. Furthermore, accuracy of finite element modeling is based on the accurate tissue properties being assigned. Temperature changes in living tissue maybe have a largely different value in the frozen state when a phase change is considered. In mass transfer modeling, a preferred model should couple the blood side transfer as well as the artery geometry, since hemodynamics has been regarded as an important factor linked to blood vessel disease.

LIST OF REFFERENCES

LIST OF REFFERENCES

[1] Rigatelli. G., and Zanchetta, M., "Interventional treatment of noncoronary atherosclerotic pathologies: and uptake about what the cadiologists should know," Ital. Hear J., 2004, Vol. 5, pp 99-113.

[2] Bhargava, B., Karthikeyan, G., Abizaid, A. S., and Mehran, R., "New approaches to preventing restenosis," British Medical Journal, Aug 2003, Vol. 327, pp 274-279.

[3] Fava, M., Loyola, S., Polydorou, A., Papapavlou, P., Polydorou, A., Mendiz, O., and Joye, J. D., "Cryoplasty for Femoropopliteal Arterial Disease: Late Angiographic Results of Initial Human Experience," Journal of Vascular and Interventional Radiology, 2004, Vol. 15, pp 1239-43.

[4] Mauro, M. A., "The battle of intimal hyperplasia in the war against femoropopliteal disease," Radiology, 2004, Vol. 231, pp 299-301.

[5] Stary, H. C., Blankenhorn, D. H., and Chanlder A. B., "A definition of the intima of human artery and of its atherosclerosis prone region," Circulation, 1992, Vol. 85, pp 391-405.

[6] Raymod, P. V., and Stancey, A. D., "Blood vessel constitutive modes: 1995-2002," Annu. Rev. Biomed. Eng., 2003, Vol. 5, pp 413-39.

[7] Ross, R., "The pathogenesis of atherosclerosis: a perspective for the 1990s," Nature, April 1993, Vol. 362, pp 801-9.

[8] Hegele, R. A., "The pathogenesis of Atherosclerosis," Clin. Chim. Acta., 1996, Vol. 246, pp 21-38.

[9] Westhuyzen, J., "The oxidation hypothesis of atherosclerosis: an update," Annals of Clinical and Laboratory Science, 2002, Vol. 27, pp 1-10.

[10] Libby, P., Ridker, P. M., and Maseri A., "Inflammation and Atherosclerosis," Circulation, 2002, Vol. 105, pp 1135-37.

[11] Xiaosong, W. and Beverly, P., "Comparative genertics of atherosclerosis and restenosis with mouse models," Arteriosclerosis, Thrombosis, and Vascular Biology, 2002, Vol. 22, pp 884.

[12] Saproval, M. R., Long, A. L., Rayanud, A. C., Beyssen, B. M., Fiessinger, J. N., Gaux, J. C., " Femoropopliteal stent placement: long term results," Radiology, 1992, Vol.

184, pp833-839.

[13] Gage, A. A., Fazekas, G., Riley E. E., “Freezing injury to large blood vessels in dog with comments on the effect of experimental freezing of bile ducts,” Surgery, 1967, Vol. 61, pp 748-754.

[14] Gage, A. A., “Selective Cryoptherapy,” Cell Preservation Technology, 2004, Vol. 2, pp 3-14.

[15] Hollister, W. R., Baust, J. M., Buskirk R. G., “ Cellular components of the coronary vasculature exhibit differential sensivity to low temperature insult,” Cell Preservation Technology, 2003, Vol. 1, pp 269-280.

[16] Cheema A. N., Nili, N., Li C. W., “ Effects of intravascular cryotherapy on vessel wall repair in a balloon injuryed rabbit iliac artery model,” Cardiovasc. Res., 2003, Vol. 59, pp 222-223.

[17] Joye, D., Tatsutani, K., “In vivo study of endovascular cryotherapy for prevention of restenosis, “ (http://www.cryoinc.com/pages/images/invivo_whitepaper.pdf)

[18] Terashima, M., Honda, Y., Goar, F. S., Joye, J. D., Tatsutani, K., Yoklavich, M., Yock, P. G., Fitzgerald, P. J., “ Feasibility and safety of a novel crypangioplasty system, J. Am. Coll. Cariol. 2002, Vol. 39, pp 57.

[19] Pennes, H. H., “Analysis of tissue and arterial blood temperatures in the resting forearm, “ J. Appl. Physiol., 1948, Vol. 1, pp 93-122.

[20] Chen, M. M., and Holmes, K. R., “ Microvascular contributions in tissue heat transfer,” Annals NY Acad. Sci., 1980, Vol. 335, pp 137-150.

[21] Weinbaum, S., Jiji, L. M., and Lemons, D. E., “Experimental studies on the role of the micro and macro vascular system in tissue heat transfer,” Am. J. Physiol., 1987, Vol 253, pp R128.

[22] Anderson, G. T., and Valvano, J. W., “A small artery heat transfer model for self-heated thermostor measurement of perfusion in the Canine Kidney Cortex,” J. Biomech. Eng., 1994, Vol. 116, pp 71-78.

[23] Wissler, E. H., “ Pennes’ 1948 paper revisited,” J. Appl. Physiol., 1998, Vol. 85, pp 35-41.

[24] Akin, H., Xu, L. X., and Holmes, K. R., “Recent Developments in Modeling Heat Transfer in Blood Perfused Tissues,” IEEE Trans. Biomed. Eng., 1994, Vol. 41, pp

97-107.

[25] Diller, K. R., and Hayes, L. J., “A finite element model of burn injury in blood-perfused skin,” J. Biomech. Eng., 1983, Vol. 105, pp 300-307.

[26] Valvano, J. W., Chitsabesan, B., 1987, “Thermal conductivity and Diffusitivity of arterial wall and atherosclerosis plaque,” Lasers in the Life Sciences, 1987, Vol. 1, pp 219-229.

[27] Welch, A. J., Valvano, J. W., Pearce, J. A. Hayes, L. J., and Aotamedi, M., 1985, “ Effect of laser radiation on tissue during laser angioplasty,” Lasers in Surgery and Medicine, 1985, Vol. 5, pp 251-264.

[28] Kleinberger, M., Oh, S., and EcElhaney, J. H., “Finite element analysis of balloon angioplasty,” Med. and Bio. Eng. And Comput., 1994, Vol. 32, pp S108-S114.

[29] Narayanaswamy M., Wright K. C., and Kandarpa K., “ Animal models for atherpsclerosis, restensosis, and endovascular Graft research,” Journal of Vascular and Intervenional Radiology, 2000, Vol. 11, pp 5-17.

[30] Topol, E. J., Leya, F., Pinkerton, C. A., Whitlow P. L., Hofling, B., Somonton, C. A., Masden, R. R., Serruys, P. W., Leon, M. B., Williams, D. O., “ A comparision of directional atherectomy with with coronary angioplasty in patients with coronary artery disease,” N. Engl. J. Med., Jul 1993, Vol. 329, pp 221-7.

[31] Wynn, R. M., “Biology of the Uterus,” New York: Plenum, 1977.

[32] Vacca, G., Battaglia, E., Grossini, D. A., Mary, C. Surico, N., ”Changes in regional blood flow in response to distension of the uterus in anaesthetized pigs,” J. Auston Nerv. Syst., 1997, Vol. 66, pp 7-14.

[33] Guretzki, H. J., Gerbilz, K. D., Olgemoller, B., Schleicher, E., “Atherogenic levels of low density lipoprotein alter the permeability and composition of the endothelial barrier,” Atherosclerosis, 1994, Vol. 107, pp 15-24.

[34] Ethier C. R., “Computational modeling of mass transfer and links to atherosclerosis,” Annals of Biomedical Engineering, 2002, Vol. 30, pp 461-471.

[35] Fletcher, C. A. J., “Computional technique for fluid dynamics,” Springer Verlag, 1999.

[36] Hose, D. R., Narracott, A. J., Griffith, S. B., Mahmood, S., Gunn, J., Sweeney, D., and Lawford, P. V., “ A thermal analogy for modeling drug elutin from

cardiovascular stents," Comp. Meth. in Biomec. and Biomed. Eng. Vol. 7, No. 5, October 2004, pp 257-264.

[37] Wada, S. and Karino, T., "Theoretical study on flow dependent concentration polarization of low density lipoproteins at luminal surface of a straight artery," Biorheology, 1999, Vol. 36, 207-223.

[38] William, C. C., and James, D. O., "Low density lipoprotein particle number and risk for cardiovascular disease," Current Atherosclerosis Reports, 2004, Vol. 6, pp 381-387.

[39] Curmi, P.A., Juan, L., Tedgui, A., "Effect of transmural pressure on low density lipoprotein and albumin transport and distribution across the intact arterial wall,' Circ. Res., 1990, Vol. 66, pp 1692-1702.

[40] Tedgui, A., Lever, M.J., "The interaction of convection and diffusion in the transport of ^{131}I-albumin within the media of the rabbit thoracic aorta," Circ. Res., 1985, Vol. 57, pp 856-863.

[41] Baldwin, A. L., Wilson, L. M., Gradus-Pizlo, I., Wilensky, R., and March, K.," Effect of atherosclerosis on transmural convection and arterial ultra structure," Thrombosis and Vascular Biology, 1997, Vol. 17, pp 3365-75.

[42] Mayer, G., Merval, R., Tedgui, A., "Effect of pressure-induce stretch and convection on low density lipoprotein and albumin uptake in the rabbit aortic wall," Cir. Res., 1996, Vol. 79, pp 532-540.

[43] American Heart Association (**http://www**.americanheart.org)

[44] Bischof, J. C., and Grassl E. D., "In vitro model system for evaluation of smooth muscle cell response cryoplasty," Cryobiology, 2005, Vol. 50, pp 162-173.

[45] Thie, M., Schlumberger, W., Semich, R., Rauterberg, J., Robenek, H., "Aortic smooth cells in collagen lattices culture: effects on ultrastructure, proliferation and collagen synthesis," Eur. J. Cell Biol., 1991, Vol. 55, pp 295-304.

[46] Berger, S. A., Goldsmith, W., Lewis, E. R., "Introduction to Bioengineering," 2004, pp 218.

[47] Xu, L. X., Chen, M. M., Holmes, K. R., Akin, H., "The evaluation of the Pennes, the Chen-Holmes, the WeinBaum-Jiji bioheat transfer models in the pig kidney cortex," ASME WAM Proc., 1991, pp 15-21.

[48] Nissen, S., "Atherosclerosis development," Clinical Cardiology, 2004, Vol. 27, pp 17-20.

[49] Young, L. A., Boehm, R. F., “A finite difference heat transfer analysis of a percutaneous transluminal microwave angioplasty system,” Journal of Biomechanical Engineering, 1993, Vol. 115. pp 441-446.

[50] Zohdi, T. I., Holzapfel, G. A., Berger, S. A., “A phenomenological model for atherosclerotic plaque growth and rupture,” Journal of Theoretical Biology, 2004, Vol. 227, pp 437-443.

[51] Steinman, D. A., Vorp, D. A., Ethier, C. R., “Computer modeling of arterial biomechanics: Insights into pathogenesis and treatment of vascular disease,” Journal of Vascular Surgery, 2003, Vol. 37, pp 1118-1124.

[52] Grundy, S. M., “Role of low-density lipoprotein in atherogenesis and development of coronary heart disease,” Clinical Chemistry, 1995, Vol. 41, pp 139-146.

[53] James, D. J., ”An overview of cryoplasty,” Endovascular Today, 2004, pp 54-56.

[54] Ozkavukcu, S., Erdemli E., “Cryopreservation: basic knowledge and biophysical effects,” Journal of Ankara Medical School, 2002, Vol. 24, 187-196.

[55] Gage, A. A., Baust J. G., “Cryosurgery: A review of recent advances current issues, CryoLetters, 2002, Vol. 23, pp69-78.

[56] Drobnis, E. Z., Crowe, L. M., Berger, T., Overstreet, J. W., “Cold shock damage is due to lipid phase transitions in cell membrane: A demostration using sperm as a model,” J. of Exp. Z., Vol. 265, pp 432-437.

[57] McGrath, J. J., “Quantitaive measurement of cell membrane transport: technology and applications,” Cryobiology, 1997, Vol. 34, pp315-334.

[58] Rubinsky, B., “Heat transfer in biomedical engineering and biotechnology,” Proceedings of ASME Thermal Engineering Conference,1999.

[59] Kimura, T., Kaburagi, S., Tamura, T., Yokoi, H., Nakagawa, Y., Yokoi, H., “Remodeling of human coronary arteries undergoing coronary angioplasty or atherectomy,” Circulation, 1997, Vol. 96, pp 475-483.

[60] Wada, S., Karino, T., “Theoretical prediction of low-density lipoproteins concentration at luminal surface of an artery with a multiple bend,” Annals of Biomedical Engineering, 2002, Vol.30, pp 778-791.

[61] Chesler, N. C., Enyinna, O. C., “Particle deposition in arteries ex vivo: effects of

pressure, flow, and waveform," Journal of Biomechanical Engineering, 2003, Vol. 125, pp 389-394.

[62] Stickler, D.,"Biofilms," Curr. Opin. Microbiol., 1999, Vol. 2, pp 270-275.

[63] Walker, J. T., Hason, K., Caldwell, D., Keevil, C W.," Scanning confocal laser microcopy study of biofilm induced corrosion on copper plumbing tubes," Biofouling, 1998, Vol. 12, pp 333-344.

[64] Notermans, S., Dormans, J. A., Mead, G. C., "Contribution of surface attachment to establishment of microorganisms in food processing plants: a review," Biofouling, 1991, Vol. 5, pp21-36.

[65] Flint, S. H., Bremer, P. J., Brooks, J. D., "Biofilms in dairy manufacturing and plant description," Biofouling, 1997, Vol. 11, pp 81-97.

[66] Escher, A., Characklis, W. G., "Modeling the initial events in biofilm accumulation," In Biofilm., 1990, pp 445-86.

[67] Wanner, O., Gujer, W., "A mutlispecies biofilm mode," Biotech. and Bioengineering, 1986, Vol. 28, pp 314-328.

[68] Characklis, W. G., Marshall, K. C., "Biofilm: A basis for an interdisciplinary approach," Biofilm, Wiley-Interscience, New York, 1990.

[69] Peyton, B. M., Characklis W. G., "Kinetics of biofilm detachment," Water Science and Technology, 1992, pp 1995-1998.

[70] Ypma, T. J., "Historical development of New-Raphson method," Siam Review, 1995, Vol. 37, pp 531-551.

APPENDICES

APPENDIX A

ANSYS DESCRIPTION AND THEORY

ANSYS is a commercial finite element program, and one of the leading solvers in this segment of commercial software. ANSYS can solve various physical problems such as stress analysis, heat transfer problems, fluid flows problems as well as magnetic field calculation. Current released version of ANSYS is ANSYS 10.0.

The graphical user interface (GUI) is activated once the ANSYS starts. GUI contains five major windows, which are the utility menu, the toolbar window, the command window, the main menu and the graphic window. CUI provides a user-friendly environment in ANSYS. Users have two options either type ANSYS command directly into the command window without using the short cut functions or use the short cuts to access various functions provided in the toolbar window for those users who are not familiar to the ANSYS commands.

A model should be created before ANSYS can generate the finite element mesh. A model of physical problem can be directly created in the ANSYS or imported from other compatible commercial CAD software such as PRO/E®. Once the model is created, the mesh is generated based on the elements chosen by user in the element type function. Besides that, various types of size control of elements are also available. At this stage, the boundary conditions may be applied using the functions in solution menu. After all the boundary conditions for the problem are defined, the solution is initiated. Once a solution is obtained, the results can be analyzed in a general processor or a time history processor. Using a general

processor, various graphics display, such as stress distribution can be generated. To obtain the solution of time dependents problems, the results can be analyzed in time history processor.

To solve the time dependent problem, ANSYS uses the Newton-Raphson method. The Newton-Raphson method is well documented in the literature. Tjalling J. Ypma gives a historical review of development of the Newton-Raphson Method in his publication [60]. Only basic idea behind the method will be presented.

The Newton-Raphson method is an interative method to finding the root of equations of the form f (x) = 0, where the f (x) is assumed to have a continuous derivative f′ . The idea of Newton-Raphson method is essentially a graphical method, which finds the tangent line of the function at the current point and uses the zero of the tangent line as the next reference point. The process is repeated until the root is found. The interative algorithm is expressed as

$$X_{i+1} = X_i - \frac{f(x_i)}{f^{'}(x_i)} \qquad \text{(A.1)}$$

The derivative of the function is often approximated by a finite difference of the form

$$f^{'}(x_i) \approx h_i^{-1}[f(x_i + h_i) - f(x_i)] \qquad \text{(A.2)}$$

Where $X_0 = X_i$ is the starting point for the interation and X_0 is a free chosen X value. Should the derivative be 0 at any point, another X_0 may be chosen to reach convergence. To avoid endless result for a poorly chosen X_0 value, usually a maximum number of interation is programmed into the numerical code.

APPENDIX B

FINITE ELEMENT FORMULATION OF PENNES BIO-HEAT EQUATION

Pennes bio-heat equation can be solved either by finite element or finite difference method. However, when an analysis is performed in complex geometries, the finite element method usually handles those geometries better than finite difference method. In he finite element method, the domain where the solution is sought is divided into a finite number of elements. Recall the Pennes bio-heat equation:

$$\rho_t c_t \frac{\partial T}{\partial t} = \nabla(k_t \nabla T) + \omega \rho_b c_b + q_m \tag{B.1}$$

Apply the method of weighted residual to equation (B.1) with a weight function, w, over a single element Ω_e , results in:

$$\oint_{\Omega_e} w\left\{ \rho_t c_t \frac{\partial T}{\partial t} - \nabla \cdot k \nabla T - \omega \rho_b c_b \left(T_b - T\right) - q_m \right\} d\Omega_e = 0 \tag{B.2}$$

Integrating equation (B.2) by parts creates the weak statement for the element

$$\oint_{\Omega_e} w \rho_t c_t \frac{\partial T}{\partial t} d\Omega_e + \oint_{\Omega_e} \left\{ \left(k \left(\frac{\partial w}{\partial x}\frac{\partial T}{\partial x} + \frac{\partial w}{\partial y}\frac{\partial T}{\partial y} + \frac{\partial w}{\partial z}\frac{\partial T}{\partial z} \right) \right) + w \omega \rho_b c_b T \right\} d\Omega_e =$$
$$\oint_{\Omega_e} w\left(\omega \rho_b c_b T_b + q_m\right) d\Omega_e - \int_{\Gamma_e} w\left(\vec{q} \cdot \vec{n}\right) d\Gamma_e \tag{B.3}$$

Here, Γ_e is the surface element. The temperature variation inside the element can be expressed by

$$T(x, y, z) = \sum_{i=1}^{m} N_i(x, y, z) T_i \tag{B.4}$$

where i is an element local node number, m is the total number of element nodes and N is the

shape function associated with node i. Using the Galerkin method, the weight function w is chosen to be the same as the interpolation function for T. With this, the weak function statement in equation (B.3) can be written in matrix form as

$$\left[C^e\right]\left\{\frac{\partial T^e}{\partial t}\right\}+\left[K_c^e\right]\left\{T^e\right\}=\left\{R^e\right\} \tag{B.5}$$

The matrix B, the local stiffness matrix $\left[K_c^e\right]$, the local capacitance $\left[C^e\right]$, and the residual vector $\left\{R^e\right\}$ for each element are given by

$$\left[B\right]=\begin{bmatrix} \frac{\partial N_1}{\partial x} & \frac{\partial N_2}{\partial x} & \cdots & \frac{\partial N_m}{\partial x} \\ \frac{\partial N_1}{\partial y} & \frac{\partial N_2}{\partial y} & \cdots & \frac{\partial N_m}{\partial y} \\ \frac{\partial N_1}{\partial z} & \frac{\partial N_3}{\partial z} & \cdots & \frac{\partial N_m}{\partial z} \end{bmatrix} \tag{B.6}$$

$$\left[K_c^e\right]=\left(k\left[B\right]^T\left[B\right]+\omega\rho_b c_b\left\{N\right\}\left[N\right]\right)d\Omega_e \tag{B.7}$$

$$\left[C^e\right]=\int_{\Omega_e}\rho c_b\left\{N\right\}\left[N\right]d\Omega_e \tag{B.8}$$

$$\left\{R^e\right\}=\int\left(q_m+\omega\rho_b c_b T_b\right)\left\{N\right\}d\Omega_e-\int_{\Gamma^e}q_s d\Gamma^e \tag{B.9}$$

Evaluation of each element in the form of equation (B.5) and then assembling into the global system equations for each node in the domain yields

$$\left[C\right]\left\{\dot{T}\right\}+\left[K_c\right]\left\{T\right\}=\left\{R\right\} \tag{B.10}$$

This set of equations can be solved with any kind on numerical integration in time to obtain the approximate temperature distribution in the domain. For example, use the Crank-Nicolson method

$$\left(\frac{1}{2}[K_c]+\frac{1}{\Delta t}[C]\right)\{T_{n+1}\}=\left(\frac{1}{2}[K_c]+\frac{1}{\Delta t}[C]\right)\{T_n\}+\frac{1}{2}\left(\{R_{n+1}\}+\{R\}\right) \tag{B.11}$$

where the subscript n+1 donates the current time step and the subscript n, the previous time step.

The steady state finite element formulation of the Pennes bio-heat equation is obtained similary to equation (B.11) and takes the form

$$[K_c]\{T\}=\{R\} \tag{B.12}$$

It is obvious from the equation (B.1) to (B.12) that, in general, the finite element formulation of the Pennes bio-heat equation resembles that of the finite element formulation of conduction heat transfer in inanimate systems. The main difference is that in the stiffness matrix, there is a term related to the volumetric blood flow in tissue and in the residual, force vector $\{R\}$, there are terms related to the arterial blood temperature and the metabolic heat generation. Stability and accuracy of numerical integration as a function of the equation matrices remains the same as in conventional inanimate heat transfer.